

# Leaping through tree space: continuous phylogenetic inference for rooted and unrooted trees

Matthew J Penn<sup>1\*</sup>, Neil Scheidwasser<sup>2\*</sup>, Joseph Penn<sup>6</sup>, Christl A Donnelly<sup>1,4,5</sup>, David A Duchêne<sup>3\*</sup> & Samir Bhatt<sup>2,5</sup> ✉

<sup>1</sup>Department of Statistics, University of Oxford, Oxford, United Kingdom; <sup>2</sup>Section of Epidemiology, University of Copenhagen, Copenhagen, Denmark; <sup>3</sup>Center for Evolutionary Hologenomics, University of Copenhagen, Copenhagen, Denmark; <sup>4</sup>Pandemic Sciences Institute, University of Oxford, Oxford, United Kingdom; <sup>5</sup>MRC Centre for Global Infectious Disease Analysis, Department of Infectious Disease Epidemiology, School of Public Health, Faculty of Medicine, Imperial College London, London, United Kingdom; <sup>6</sup>Department of Physics, University of Oxford, Oxford, United Kingdom; \*Equal contribution

**Phylogenetics is now fundamental in life sciences, providing insights into the earliest branches of life and the origins and spread of epidemics. However, finding suitable phylogenies from the vast space of possible trees remains challenging. To address this problem, for the first time, we perform both tree exploration and inference in a continuous space where the computation of gradients is possible. This continuous relaxation allows for major leaps across tree space in both rooted and unrooted trees, and is less susceptible to convergence to local minima. Our approach outperforms the current best methods for inference on unrooted trees and, in simulation, accurately infers the tree and root in ultrametric cases. The approach is effective in cases of empirical data with negligible amounts of data, which we demonstrate on the phylogeny of jawed vertebrates. Indeed, only a few genes with an ultrametric signal were generally sufficient for resolving the major lineages of vertebrate. With cubic-time complexity and efficient optimisation via automatic differentiation, our method presents an effective way forwards for exploring the most difficult, data-deficient phylogenetic questions.**

**Keywords:** phylogenetic inference | balanced minimum evolution | gradient descent | distance matrix

**Correspondence:** [s.bhatt@imperial.ac.uk](mailto:s.bhatt@imperial.ac.uk)

## Introduction

Phylogenetic inference, the task of reconstructing the evolutionary relationships across taxonomic units given observational data, has a wide range of theoretical and practical applications in the biological sciences, such as in biology [1–3] and epidemiology [4], but also in linguistics [5] and cultural anthropology [6, 7]. In particular, the COVID-19 pandemic has catalysed research efforts to develop efficient tools and methods in phylogenetics [8–14]. For biological problems, tree inference is primarily informed by molecular sequence data (i.e., nucleotide or amino acid sequences), for which an extensive body of literature exists [15–17]. Other sources of biological data such as morphology [18], fossils [19], and auditory communication in animals [20] can also be used as input. Yet despite an explosion in data available for millions of taxonomic units, as seen during the recent pandemic, we are still unable to effectively explore the gigantic parameter spaces involved during inference.

Two key parameters considered when inferring a phylogenetic tree include the *topology*, the branching pattern that specifies the evolutionary relationships between operational taxonomic units, and *branch lengths*, the amount of evolutionary divergence that occurred between the branching events. A substantial amount of research has been conducted on how to parameterise branch lengths [21, 22], especially through the use of molecular clocks [23].

Conversely, relatively little progress has been made on methods for exploring the massive spaces of possible tree topologies. This is a fundamental challenge for inference given its combinatorial complexity: for  $n$  taxa, there are  $(2n - 3)!!$  possible rooted tree arrangements. This means that even a small dataset of 10 taxa can be enumerated by 34 million unique rooted trees. Moreover, finding the optimal tree is NP-hard for all major optimality criteria (e.g., maximum parsimony [24], minimum evolution [25], maximum likelihood [26]). Methods such as linear programming [27] or branch and bound [28] can provide exact solutions, but are practically limited to problems with  $\approx 15$  or fewer taxa. To overcome these challenges, the overwhelming majority of state-of-the-art software (e.g., MrBayes [29], PAUP [30], BEAST [31], PAML [32], RAxML(-NG) [33, 34], FastME [35], IQ-TREE [36, 37]) rely on hand-engineered search heuristics to perform tree topology optimisation.

The most popular of these methods still have several limitations, and this includes heuristics based on subtree pruning and regrafting (SPR) and tree bisection and reconnection (TBR) operations, which have empirically been shown to be the best available methods for exploring tree topology space [33, 38]. First, the computational cost of such heuristic approaches scales poorly as the number of taxa increases. For instance, exhaustive exploration of single SPR operations is quadratic in complexity, and paired changes is quartic. The computational cost of SPR is further compounded by large memory requirements for tracking the changes from one iteration to the next. Second, all the aforementioned tree arrangements are prone to convergence to poor local minima [39] due to the inability of heuristic operations to provide sufficient directions of

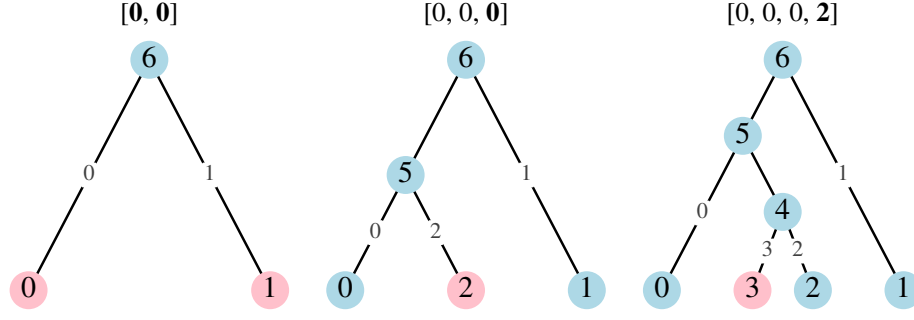


**Figure 1.** An example of the left-to-right construction of the ordered tree  $v = [0, 0, 0, 2]$ .

change to a better tree. This phenomenon is exacerbated when concatenating multiple genes in a supermatrix approach [40, 41], and when using genomic-scale data sets that lead to further computational demands.

We address these shortcomings by proposing a new paradigm for tree topology inference, expanding the problem space using a continuous rather than discrete parameterisation of a phylogenetic tree. To our knowledge, aside from considering metrics (e.g., distances in tree space) [42–44], performing topological search in a continuous tree space has not been attempted. Furthermore, very few approaches have made use of gradient-based tree proposals [43, 45, 46]. Although maximum likelihood and Bayesian inference criteria are more popular and generally considered state-of-the-art [29–31, 33, 37, 47], our framework optimises tree topology under a balanced minimum evolution (BME) criterion [48, 49] using dissimilarity matrices as an input. This criterion is well-principled [50] theoretically can match the performance of maximum likelihood approaches [51]. This framing of the minimum evolution criterion [50, 52] has also been proven to be statistically consistent [2, 53] and has repeatedly shown outstanding performance in a range of settings [35, 54–56].

To better explore the space of possible trees, we expand the space over which we need to search. Consequently, we use a continuous representation of a phylogenetic tree [57] to greatly improve the ability to search parts of this space. Appealing to a common analogy that casts the optimal tree search problem as finding a needle in a haystack, our approach observes a much bigger haystack, but the hay is in very large bundles, many of whom have a needle, and for these bundles we have access to a (weak) magnet. Providing details to this analogy, the size of the usual phylogenetic haystack with  $n$  taxa is  $(2n - 3)!!$  [58], while we search a much larger haystack of size  $(n!)^2$ . There are  $n!$  bundles in this larger haystack, each of which contains  $n!$  trees, but for any tree,  $2^{n-1}$  bundles will contain that tree. Although the proportion of bundles containing a needle shrinks exponentially, we propose a novel approach (Queue Shuffle) that chooses bundles that should be closer to one with a needle. For any given bundle, we also introduce a continuous objective function that can be efficiently traversed using gradient descent approaches (the

weak magnet) developed for large-scale machine learning problems [59–61]. This continuous objective facilitates enormous changes to tree topology in a single step in a direction that improves the objective function. After searching any given bundle using the continuous objective, we use Queue Shuffle, which improves the switch towards the next bundle to search. Our counterintuitive approach, called GradME, offers a powerful alternative to the existing heuristic methods used for topological inference, outperforming the current state-of-the-art with an overall complexity comparable to neighbour joining ( $\mathcal{O}(n^3)$ ).

## Methods

**An ordered bijection to tree space.** Previously, we introduced Phylo2Vec [57], a novel bijection between the space of trees and a space of integer vectors. In contrast to other bijections such as Prüfer codes [62] or permutation matchings [63], changes in Phylo2Vec correspond to smooth changes in the tree space, e.g., single changes in a Phylo2Vec vector correspond to a limited set of SPR changes.

Here, we focus on the notion of *ordered trees* from [57], where it is possible to construct a tree from its vector in linear ( $\mathcal{O}(n)$ ) time. An ordered tree can be thought of as a birth process, where when a birth occurs, the original node continues to live and retains its label, while the new node receives an incremented label. Accordingly, we introduce an equivalent but more intuitive tree construction process for these ordered trees. We begin with two leaf nodes and two edges labelled 0 and 1. We then append nodes by joining them, *in order*, to edges connecting leaf nodes to the tree. In Fig. 1, we first append node 2 to its label edge 0, creating a new internal node and a pair of new edges. The new edge joining node 2 to the tree is labelled as edge 2. We then append node 3 to edge 2, again creating a new internal node and two new edges. This tree construction process can be summarised by a single vector  $v$ , with  $v_0 = v_1 = 0$  and, for  $m \geq 2$ ,  $v_m$  being the label of the edge to which node  $m$  is appended. Each index in  $v_m$  is subject to

the simple constraint:

$$\begin{aligned} v_0 &= v_1 = 0 \quad \text{and} \\ v_m &\in \{0, 1, \dots, m-1\} \quad \forall \quad m \geq 2 \end{aligned} \quad (1)$$

which is equivalent to the definition of ordered trees in [57]. It is proved in Appendix C that for ordered  $v$ , the algorithm presented above and the more general algorithm in [57] produce equivalent trees.

**A continuous representation of a tree.** We introduce a square matrix  $W$  which gives the distribution of a random ordered vector  $V$  with independent entries such that  $W_{ij} = \mathbb{P}(V_i = j)$ . Given Eq. 1,  $W$  is a lower-triangular, stochastic matrix (row sums to 1).  $W$  is designed to be a continuous representation of a phylogenetic tree, and can probabilistically represent any *ordered* phylogenetic tree (a space of  $n!$  trees). A simple approach to determining the best single tree from  $W$  is to take the column-wise argmax, yielding a single tree  $v$ .

**Queue Shuffle: changing orderings to explore all the tree space.** The number of ordered trees,  $n!$ , is substantially smaller than the possible number of trees,  $(2n-3)!!$  (although with a comparable growth pattern in  $n$ ), and hence, the optimal ordered tree is likely to be close to, but not exactly equal to, the true optimal tree.

To fully explore tree space, we randomly change the labels of the leaf nodes in the optimal ordered tree using a novel approach we call the *Queue Shuffle* (full details in Appendix G). Shuffling amounts to choosing a permutation  $\sigma$  on  $\{0, 1, \dots, n-1\}$  such that the leaf with name  $N_i$  now has label  $\sigma(i)$ . We call this an *ordering* of the leaf nodes.

Each different ordering changes the explorable space of ordered trees. Thus, once an ordering is chosen, one can re-optimize an objective function  $F(W)$  in this new space of ordered trees (note that the previous optimal tree is still in this space and so, provided it finds the true optimal ordered tree, it will have an objective value no worse than the previous tree). This process is then repeated, re-ordering the tree and re-optimizing in the new space, until the best found tree does not change for a certain number of iterations. In practice, only ten to twenty iterations are needed from some random starting order, and less if a sensible start (such as from a neighbour joining tree) is used.

A given tree is in the space of ordered trees for at least  $2^{n-1}$  orderings. This means that we do not need to find a single optimal ordering, but have exponentially many which will return the true optimal tree. Very loosely considered, being able to explore  $n!$  tree space reliably and efficiently with continuous optimisation, Queue Shuffle reduces the inferential task to one that is exponential.

**Why does Queue Shuffle work?** While the number of optimal orderings grows exponentially, their proportion tends quickly to zero as  $n$  grows. It is therefore, perhaps, surprising that we are able to find an optimal ordering so quickly from merely tens of shuffles. The proportion of optimal orderings (approximately the ratio of ordered trees to total trees,  $\frac{(n-1)!}{(2n-3)!!}$ ) ranges from  $8 \times 10^{-4}$  in our smallest dataset (14 taxa) to  $6 \times 10^{-29}$  in the largest (99 taxa).

However, our algorithm is able to find these optimal orderings because the Queue Shuffle does not choose the new ordering uniformly over the space of orderings (which is  $n!$  large). Instead, the distribution depends on the structure of the tree and therefore facilitates sensible proposals. For example, nodes which are close to the root are always given low labels, meaning that they will also be close to the root in a high proportion of the trees in the new space of ordered trees (cf. Appendix G).

When a good tree is found in some ordered space, it is reasonable to expect a better tree will retain similarities with the good tree, and the Queue Shuffle allows for these trees to be explored. Theorem 1 in Appendix G formalises the *swapping property* of the Queue Shuffle, illustrated in Fig. 2. Given any pair of subtrees which are connected to the tree by two nodes that share an edge, the swapping property states that, with at least probability  $\frac{1}{4}$ , a tree that is identical to the previous optimum, with the exception that these two subtrees are swapped, will be in the new space of ordered trees. This ensures that this new space contains many sensible proposal trees. Moreover, the fact that this probability is bounded below by a fixed constant, independent of the size of the phylogeny, is a surprising, and powerful property: it means that there is a sense of continuity when moving between ordered tree spaces.

**Balanced minimum evolution.** Popular objective functions for inferring the best tree given some data include maximum parsimony [64], maximum likelihood [65] and minimum evolution [66]. Of these three, only maximum likelihood and minimum evolution are provably statistically consistent [2, 53] (maximum parsimony can be inconsistent under certain conditions [67]). For small to moderate sized phylogenies, maximum likelihood (and Bayesian extensions) is generally considered state-of-the-art [30, 31, 33, 37], but approaches based on minimum evolution have also consistently shown to yield comparable performance [26, 35, 54–56]. The first introductions of the minimum evolution paradigm [50, 52] sought to express evolutionary relationships through dissimilarity. They proved that, given unbiased estimates of the true evolutionary distances, the true phylogeny has an expected length shorter than any other possible phylogeny – thereby establishing a principled objective criterion. Currently, the best performing minimum evolution approach is that of balanced minimum evolution (BME) [48, 49] (with the widely used software implementation FastME [35]). Given  $D_{ij}$ , the

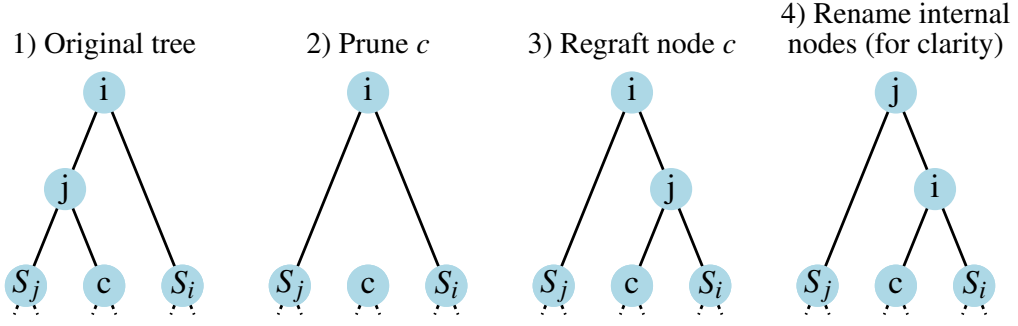


**Figure 2.** A simple representation of the swapping property of Queue Shuffle. The swapped subtrees have roots labelled  $S_i$  and  $S_j$  while the node label  $c$  is the subject of the equivalent subtree-prune and regraft operation. Note that in step 4, the internal nodes are renamed to illustrate that the required swap has indeed occurred.

distance between two taxa  $i, j$ , (where this distance could be based on morphology, molecular sequences etc.) and  $e_{ij}$ , the number of branches in the path between taxa  $i$  and  $j$  (the path length [68]), the objective function for a given tree  $T$  is:

$$\mathcal{L}(T) = \sum_{i,j} D_{ij} 2^{-e_{ij}} \quad (2)$$

This objective can be computed in a numerically stable fashion using the log-sum-exp trick. A widely used approach to estimate the optimal tree greedily [53, 56] is the neighbour joining method [66]. When neighbour joining is based on an additive distance measure, it reconstructs a unique tree, but still performs well with near-additive trees [69] and under small perturbations in the data [70]. However, despite these highly favourable properties, further heuristic optimisation on a neighbour joining tree utilising subtree-prune and regrafting have proven to be even more accurate [35]. Once a tree topology is found, quadratic algorithms exist for estimating the branch lengths [71] as well as efficient approaches for molecular clock dating [72].

**Balanced minimum evolution for rooted trees.** Inference using BME is almost always restricted to unrooted trees [68] with rooting chosen after inference through heuristics (e.g., midpoint rooting) or via a molecular clock (e.g., for serially sampled data). However, it is often of interest to find the optimal rooted tree for a set of taxa, as this provides extra biological context.

In an unrooted tree, the BME objective function (Eq. 2) provides an efficient way of calculating the total length of a tree where the branch lengths are the least squares estimators for approximating each  $D_{ij}$  with the distance from nodes  $i$  to  $j$  in the tree. However, this result does not hold in a rooted tree, as the addition of a root changes some path lengths.

To remedy this, we consider adding a hypothetical and very distant, root (as node  $n$ ) into the tree and finding the optimal unrooted tree with these  $n + 1$  taxa. We can create

a rooted tree by removing node  $n$  and, as we know that node  $n$  evolved first, this will be the root of the original  $n$  taxa. Moreover, we show in Appendix B that, to leading order, the BME objective applied to this rooted tree differs only by a constant from the BME objective applied to the unrooted tree with  $n + 1$  taxa. Thus, BME provides a sensible method for finding the optimal rooted tree and can be sensibly applied directly to a rooted topology. However, as discussed in detail in Appendix B, it will struggle to find the correct root of trees that are not ultrametric as the root will be drawn towards taxa that are more distant from the root.

#### Gradient-based optimisation using the BME criterion.

Defining  $f(v)$  to be the BME objective function for the tree generated by  $v$ , we then create a continuous objective,  $F(W)$  by  $F(W) = \mathbb{E}[f(V)]$ . We present in Appendix E a novel method for calculating this objective function in cubic time ( $\mathcal{O}(n^3)$ ; where  $n$  is the number of taxa). We can perform inference on this objective for both rooted and unrooted trees.

An important property of our continuous objective function is that there is always a minimum at a “discrete tree” – that is, at a matrix  $W$  where for each row, one value is 1 and all the others are 0 (e.g., see Fig. 3a). Moreover, the objective function is a polynomial function of the entries of  $W$  and is linear in each fixed entry (that is, the diagonal entries of  $\nabla^2 F$  are zero), making it easy to differentiate analytically, numerically or automatically. Using state-of-the-art automatic differentiation [73], gradient descent can be used to efficiently minimize  $F$  and find the optimal *ordered* tree.

We refer the resulting system, combining the continuous tree representation, Queue Shuffle reordering, and the gradient-based optimisation framework using BME, as **GradME**.



**Table 1.** Evaluation datasets. rRNA/rDNA: ribosomal RNA/DNA, mtDNA: mitochondrial DNA. AA: amino acid. For the Jawed dataset, several subsets of the original dataset [74] were used (from 1,460 to 18,406 sites; cf. Fig. 3c).

Dataset	Reference	# Sites	# Taxa	Type	Taxonomic rank
DS1	[75]	1,949	27	rRNA (18S)	Tetrapods
DS2	[76]	2,520	29	rRNA (18S)	Acanthocephalans
DS3	[77]	1,812	36	mtDNA	Mammals; mainly Lemurs
DS4	[78]	1,137	41	rDNA (18S)	Fungi; mainly Ascomycota
DS5	[79, 80]	378	50	DNA	Lepidoptera
DS6	[81]	1,133	50	rDNA (28S)	Fungi; mainly Diaporthales
DS7	[82]	1,824	59	mtDNA	Mammals; mainly Lemurs
DS8	[83]	1,008	64	rDNA (28S)	Fungi; mainly Hypocreales
DS9	[84]	955	67	DNA	Poaceae (grasses)
DS10	[85]	1,098	67	DNA	Fungi; mainly Ascomycota
DS11	[86]	1,082	71	DNA	Lichen
Eutherian	[87]	1,338,678	37	DNA	Eutherian Mammals
Jawed	[74]	1,460-18,406	99	AA	Gnathostomata (jawed vertebrates)
Primates	[88, 89]	232	14	mtDNA	Mammals; mainly Primates

**Evaluation.** We evaluate GradME on a diverse corpus of 14 empirical molecular sequence datasets (Table 1). The first 11 are commonly used to assess phylogenetic inference performance [90], whereas the last three were used to assess inference on rooted trees. For each dataset, we start from a random tree and optimise the  $W$  matrix to a tolerance of  $1e-10$  using gradient descent with Adafactor [61] optimisation. The distance matrix  $D$  is computed using the F81 substitution model for DNA [91], and LG [92] for amino acids. Jukes-Cantor [93] and TN93 [94] models were also considered for DNA, while stochastic gradient descent (SGD), RMSprop [95], and AdamW [59, 60] were also considered for optimisation (see Fig. S2). As a baseline, we compute the mean BME loss over 50 random uniform trees, sampled using Phylo2Vec [57]. To fairly assess the performance of GradME, we compare our framework to two well-established distance-based methods: BioNJ [96], based on the neighbour joining algorithm [97], and FastME [35], based on balanced minimum evolution.

**Implementation.** Implementation of the BME criterion and of the optimisation framework was written in Python using Jax [73] and Optax [98]. Optimisation was performed on a Xeon 2.30GHz (CPU; Intel Corporation) or on a single GeForce GTX 1080 (GPU; Nvidia Corporation). Evaluation of the BioNJ [96] and FastME [35] methods was performed via the R package ape [89] using rpy2 [99]. Tree manipulation and visualisation scripts were written using ete3 [100] and NetworkX [101]. An implementation is available at: <https://github.com/Neclow/GradME>.

## Results

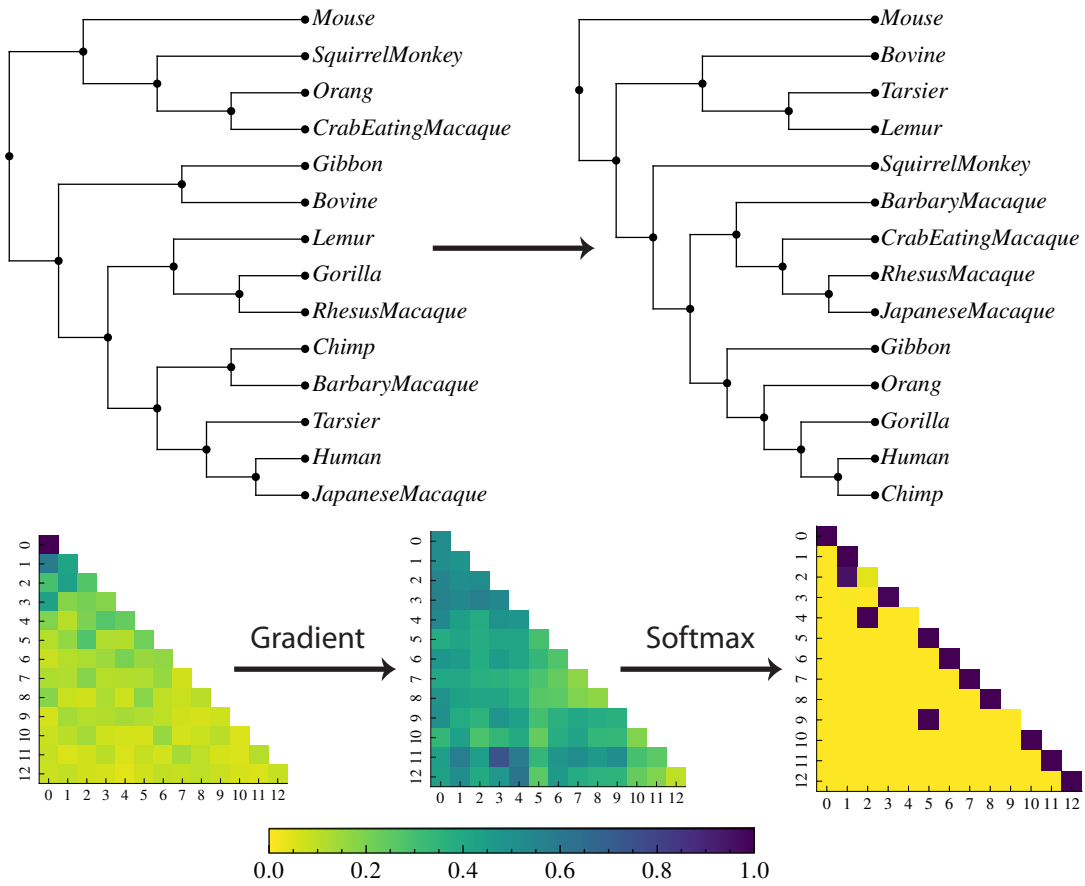
**Tree traversal in continuous space.** For any choice of label ordering, our approach admits a continuous gradient across  $n!$  trees for  $n$  leaves. This gradient, which can be

obtained readily via automatic differentiation, can rapidly traverse tree space to find trees with a close to optimal objective value. Fig. 3a shows a single gradient step for the small Primates dataset [32, 89]. Simply subtracting the gradient from a random initial tree, followed by softmax activation, results in an almost discrete  $W$  which corresponds to the best BME tree for an F81 [91] substitution model. The jump taken corresponds to six subtree-prune and regraft moves [89].

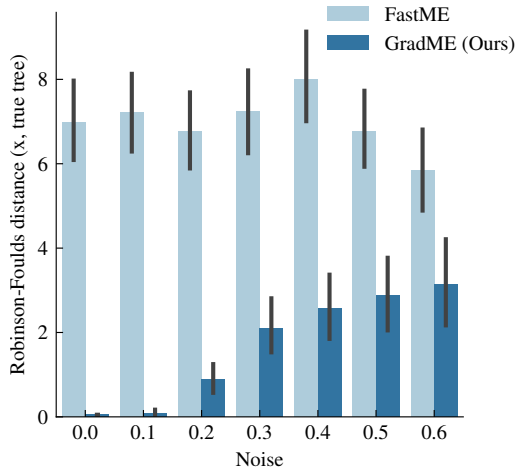
For larger alignments such as the popular Eutherian dataset [87], a single gradient step can result in 14 to 18 SPR moves. For comparison, picking any *single* subtree-prune and regraft move from the space of possible moves in a heuristic search requires  $\mathcal{O}(n^2)$  moves. We note that the gradient step size is dependent on the data and, as expected, greatly reduces as we approach an optimum.

**A comparison to benchmark phylogenetic data sets.** Table 2 presents a comparison of GradME with neighbour joining (BioNJ) and FastME (subtree-prune and regraft version) over 11 popular phylogenetic benchmark datasets [90]. Both neighbour joining and FastME are only able to infer a minimum length unrooted tree, and therefore we compare estimates only on unrooted trees. We always initialise our algorithm with a uniform, equiprobable tree, where the starting label order is either derived from Neighbour-Joining or FastME, or from a random start and optimised using Queue Shuffle. Using Queue Shuffle therefore optimises tree topology with no sensible initial guesses. As expected, FastME consistently outperforms BioNJ, with lower BME loss on all but one alignment. Starting from an ordering implied by BioNJ but optimising from a uniform starting tree, our algorithm matches BioNJ for three datasets but performs substantially better for the eight others. These results suggest a useful application of our algorithm is simply to improve on the greedy

**(a) Dataset: Primates**



**(b) Dataset: Simulated (20 taxa, 100k sites)**



**(c) Dataset: Jawed**

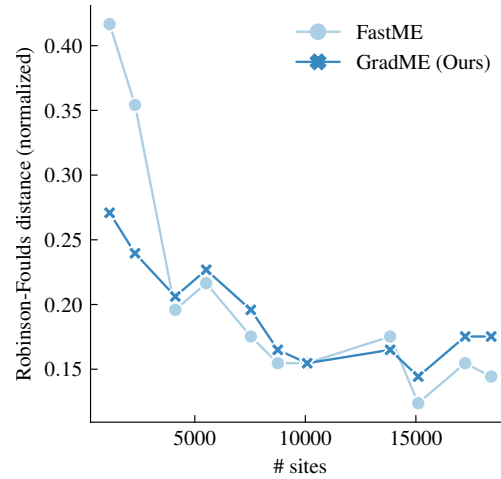


**Figure 3.** Results on empirical data **(a)** Starting from a random tree, represented by an  $n \times n$  stochastic matrix, we compute the continuous gradient, apply softmax activation and increment the original matrix. In a single step, our gradient finds the correct tree at a distance of 6 subtree-prune and regraft moves from the random starting tree. **(b)** Simulating ultrametric trees of 20 taxa and 100,000 sites under an LG model of protein evolution. We add random uniform noise to all branch lengths to simulate departures from ultrametricity. Compared to the true tree via Robinson-Foulds distance, light blue bars are midpoint rooting the best FastME tree and dark blue bars are the inferred root from our approach. **(c)** Phylogenies for jawed vertebrates, where the number of genes (hence sites) are reduced to be more clocklike. Normalised Robinson-Foulds distance are shown between the best ASTRAL [102] tree, the best unrooted FastME tree which has been midpoint rooted (light blue) and our inferred rooting algorithm (dark blue). Performance for FastME reduces when the number of sites is small

**Table 2.** Log balanced minimum evolution loss scores for 11 phylogenetic benchmark datasets. Lower is better. Scores from BioNJ and FastME were obtained following the implementations in `ape` [89]. Our approach always starts from a random uniform tree, but requires a taxon labelling ordering. We show the performance of our approach starting from a BioNJ ordering, FastME ordering, and a random ordering, optimised by Queue Shuffle. The baseline was obtained by uniformly sampling 50 random trees and obtaining their BME loss (shown: mean  $\pm$  SD). The best performing approaches for each dataset are denoted in bold.

Dataset	Baseline	No ordering		With ordering		GradME (ours)
	Random tree	BioNJ	FastME	BioNJ	FastME	
DS1	-0.609 $\pm$ 0.043	-1.18334	<b>-1.19145</b>	-1.18334	<b>-1.19145</b>	<b>-1.19145</b>
DS2	1.279 $\pm$ 0.021	0.97379	0.97408	0.97379	0.97408	<b>0.97349</b>
DS3	1.586 $\pm$ 0.023	1.23596	<b>1.23567</b>	1.23589	<b>1.23567</b>	<b>1.23567</b>
DS4	1.132 $\pm$ 0.020	0.67644	<b>0.67430</b>	0.67565	<b>0.67430</b>	<b>0.67430</b>
DS5	1.708 $\pm$ 0.014	1.32536	<b>1.32003</b>	1.32381	<b>1.32003</b>	<b>1.32003</b>
DS6	0.366 $\pm$ 0.024	-0.48565	-0.48739	-0.48715	-0.48739	<b>-0.48886</b>
DS7	1.947 $\pm$ 0.020	1.29616	<b>1.29433</b>	1.29616	<b>1.29433</b>	<b>1.29433</b>
DS8	1.029 $\pm$ 0.017	0.26538	<b>0.25609</b>	0.26294	<b>0.25609</b>	<b>0.25609</b>
DS9	-0.161 $\pm$ 0.022	-0.97842	<b>-0.97989</b>	-0.97860	<b>-0.97989</b>	<b>-0.97989</b>
DS10	0.892 $\pm$ 0.017	0.09618	<b>0.09334</b>	0.09483	<b>0.09334</b>	<b>0.09334</b>
DS11	1.152 $\pm$ 0.032	-0.07904	<b>-0.08090</b>	-0.07985	<b>-0.08090</b>	<b>-0.08090</b>

balanced minimum evolution heuristic from a starting Neighbour-Joining tree. When starting from the ordering implied from the best tree from FastME, our algorithm achieves the same minimum, suggesting that, unlike BioNJ, FastME reliably converges to a local minimum – that is, a tree with a better objective value than those “close” to it. Finally, implementing Queue Shuffle on a random starting order and from a uniform starting tree always achieves the best loss, and in two cases, finds a minimum smaller than FastME. For these analyses, we use an F81 substitution model with no Gamma correction to ensure simplicity, but we note performance does vary with the choice of substitution model. However, GradME does not perform worse than FastME, and always achieves a better or equal loss. Finally, we note that FastME’s performance is generally worse when using the nearest neighbour interchange heuristic (instead of the SPR-based heuristic).

**Rooting ultrametric trees.** Despite being applicable to the unrooted problem, our approach, at its core, works with rooted trees. As previously discussed, if we assume the existence of a distant outgroup, then the balanced minimum evolution objective can be used to optimise a rooted phylogenetic tree. In Appendix B, we show that, given an ultrametric unrooted tree, the optimal rooting maximises a heuristic for the root-to-tip distance in the tree. Equivalently, the optimal rooting ensures that the root is estimated to be the maximal possible distance back in time. This is not an immediately biologically plausible objective for the root. Indeed, the cornerstone of balanced minimum evolution is finding the tree of minimum length, and it hence seems counter-intuitive to require the root that is the maximum distance backwards in time (though this does in fact minimise the tree length). However, our assumption of a

distant ancestor means that the root of our tree must be the point that is furthest backwards in time. In particular, this means that the evolutionary direction needs to be away from the root. By setting our root such that the root-to-tip distance is maximised, we ensure that the root satisfies this constraint. However, this property does not hold for trees that are not ultrametric – in these cases, the root will be drawn towards branches with higher mutation rates.

While this property only holds for ultrametric trees, our approach still works well for near clock-like trees. As an example, we draw small (20 taxa) random ultrametric phylogenies with a total length of one, and simulate 100,000-residue protein sequences [89] down these trees under an LG [18] model of protein evolution, assuming random uniform amino acid base frequencies. In the ultrametric cases, all taxa are equidistant to the root, which corresponds to a strict molecular clock. We add uniform noise to all branch lengths to simulate departure from a strict clock. Fig. 3b shows the Robinson-Foulds [103] distance from the true tree to the *midpoint-rooted* best *unrooted* subtree-prune and regraft FastME tree, and the distance to our inferred rooted tree. We see that when the tree is ultrametric, or close to ultrametric, our approach recovers the correct rooted tree. As expected, an increase in noise leads to a decrease in topological accuracy, although our approach still performs substantially better than midpoint rooting. We note that uniform noise is unlikely to be biologically realistic. Instead, deviations from a strict clock are more likely to be heterogeneous in certain clades or internal branches. However, for small departures, we believe our algorithm to reliably infer the correct tree and root simultaneously.

We implement our rooting algorithm on the popular mammal data from [87]. We infer a rooted tree via Queue

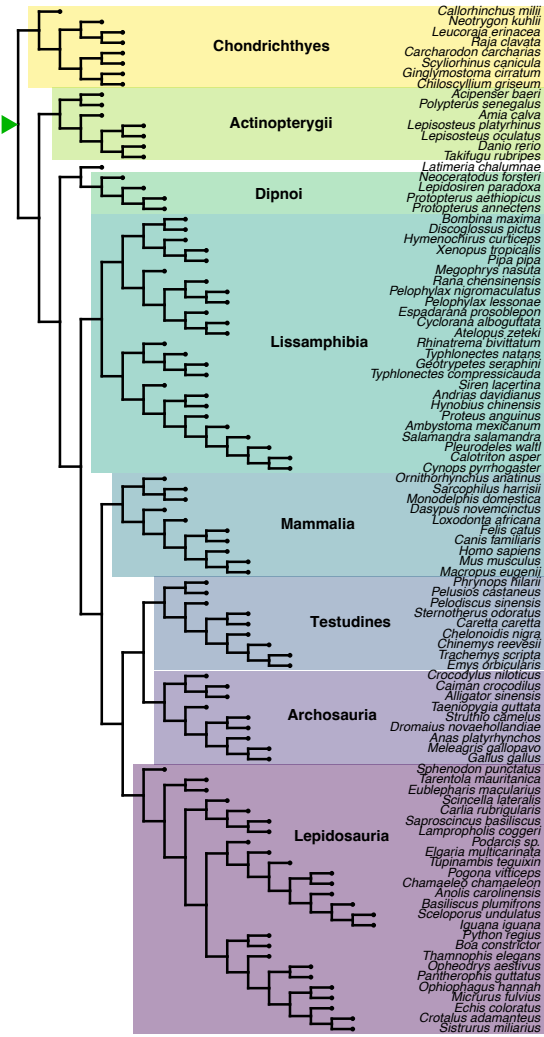
Shuffle and also midpoint root the best FastME tree. Both trees, unrooted, have the same balanced minimum evolution loss, but our rooted loss is less than the FastME midpoint rooted loss. Our rooted tree correctly identifies *Gallus gallus* (red junglefowl) as the outgroup, while midpoint rooting pairs *Gallus gallus* with *Ornithorhynchus Anatinus* (platypus) (see Fig. S1 for the rooted phylogenies).

**Rooting the phylogeny of all jawed vertebrates.** To perform a more detailed evaluation of our framework, we tested GradME's robustness for topological inference by finding the root of the large Jawed dataset with 99 taxa and 4593 genes [74]. Given the reliance of our method on ultrametric data for inference of the root, we first made a fast measure of the ultrametricity of each gene-tree. To do this, we inferred the phylogeny of each gene using FastME, followed by midpoint rooting. The coefficient of variation in root-to-tip lengths was taken as a measure of ultrametricity. We then concatenated ranked genes into supermatrices including decreasing numbers of genes, and examined the performance of FastME against our method. All inferences were performed using the LG amino-acid substitution model to maintain simplicity. We placed special focus on our ability to use small portions of data for recovering the main groupings of vertebrates; these key groupings include the root separating cartilaginous (Chondrichthyes) versus boned vertebrates, ray-finned fishes (Actinopterygii), and the major groups of tetrapods and amniotes (amphibians, mammals, archosaurs, turtles, and lizards and relatives).

Strikingly, small numbers of genes with an ultrametric signal were generally sufficient for resolving many of the major lineages of vertebrates using both FastME and our approach (Fig. 3c). However, at the smallest numbers of genes (0.05%, 2 genes), FastME was unable to recover many of the early relationships among vertebrates, such as the root, monophyly of cartilaginous fishes, ray-finned fishes, Tetrapoda, or the mammals. Even small amounts of data (1460 amino-acids of 1,964,439; 0.07% of the original data) were sufficient for GradME to resolve the root as well as every major grouping of jawed vertebrates accurately (Fig. 4). The only exception was the controversial position of the Coelacanth, which was found to be sister of Dipnoi (lungfish) rather than the more widely accepted position as sister of Dipnoi plus Tetrapoda. While this remarkable performance under the simple LG model is in part attributed to the informative nature of highly ultrametric genes, our tree topology demonstrates the superiority of our approach in accuracy and efficiency over other fast methods in phylogenetics.



A. Ours



B. FastME

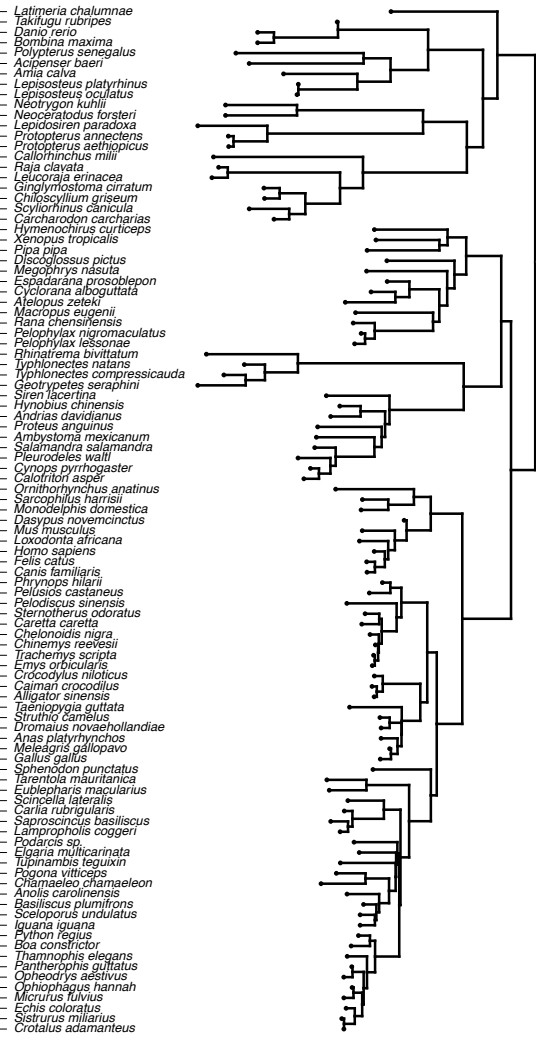


**Figure 4.** Phylogenetic inferences of the jawed vertebrates’ phylogeny using the two most ultrametric loci from a data set of 99 taxa and 4593 genes [74]. (a) Inference using our approach leads to high accuracy in identifying the root and all major jawed vertebrate taxa. Note that, we do not estimate branch lengths, but only topology via balanced minimum evolution (b) inference using FastME and midpoint rooting leads to widespread error, primarily and critically near the root of the process.

## Discussion

We have introduced a new approach for exploring the vastness of tree space. Counterintuitively, our approach explores a much bigger space than the space of possible trees, but this larger space allows for new ways to find the best tree. The key to our method’s success lies in transforming the phylogenetic tree search problem from a discrete to a continuous one, allowing us to achieve superior performance. To our knowledge, this is the first time a continuous, differentiable objective function for the inference of tree topology has been proposed, and it opens new possibilities for phylogenetic inference. Bayesian phylogenetics can be regarded as the most robust framework for inferring phylogenies, but has been to-date limited by the poor ability of random walk Metropolis-Hastings algo-

gorithms to explore tree space [104]. More efficient Hamiltonian Monte Carlo samplers have been proposed [43] to tackle this problem, and our framework presents a new avenue to jointly explore topology and branch lengths with efficient samplers. A remaining limitation of our approach is the need to shuffle labels to fully explore the space of all possible trees, and while the approach we use, Queue Shuffle, is mathematically and practically powerful, this step is still discrete. The possibility of permutation distributions such as the Gumbel-Sinkhorn could allow for a fully differentiable algorithm. Finally, the complexity of our approach is  $\mathcal{O}(n^3)$ , which easily allows for large phylogenies in the thousands, not for tens of thousands. However, computation on GPUs or TPUs in parallel can facilitate computational tractability.

A major benefit of our approach is that it naturally enables

the estimation of the root node, which has been a long matter of interest in the biological sciences [105–107]. For genes where a strict clock is a reasonable assumption, our method of traversing tree space in large steps reliably estimates both the correct tree topology and the root. Our approach will likely be useful in settings where genetic sequences are contemporaneous and time for measurable evolution is short, such as early epidemics or nosocomial settings. However, as we showed analytically, our approach will have reduced performance when considering rate heterogeneity and departures from a strict clock.

Tests on the relationships among jawed vertebrates demonstrate that even minimal amounts of data can be sufficient for our method to reach high accuracy in topology and root estimates. These results are consistent with previous work on large amounts of genome-scale data showing that clocklike loci to be the most suitable for phylogenetic inference [108]. Furthermore, our approach is effective with negligible amounts of data – where other methods are ineffective – making it a powerful addition to the existing toolkit for addressing recalcitrant questions of the tree of life.

Our approach is based on the minimum evolution principle, which has repeatedly shown to produce fast and accurate inference. Nonetheless, an interesting area for further study is to extend the continuous path length formulation to approximations of traditional phylogenetic likelihoods [65]. This would be particularly beneficial for implementation in Bayesian inference, since tree topology inference is a major obstacle to large hierarchical models [109, 110]. Our method is therefore a step towards more efficient sampling of the complex posterior distributions over tree topology.

## Data availability

All code relevant to reproduce the experiments is available online: <https://github.com/Neclow/GradME>.

## References

1. Cavalli-Sforza, L. L. & Edwards, A. W. Phylogenetic analysis. Models and estimation procedures. *Am. J. Hum. Genet.* **19**, 233 (1967).
2. Felsenstein, J. *Inferring phylogenies* (Sinauer associates Sunderland, MA, 2004).
3. O’Meara, B. C. Evolutionary inferences from phylogenies: a review of methods. *Annu. Rev. Ecol. Syst.* **43**, 267–285 (2012).
4. Grenfell, B. T. *et al.* Unifying the epidemiological and evolutionary dynamics of pathogens. *Science* **303**, 327–332 (2004).

5. Mace, R. & Holden, C. J. A phylogenetic approach to cultural evolution. *Trends Ecol. Evol.* **20**, 116–121 (2005).
6. Collard, M., Shennan, S. J. & Tehrani, J. J. Branching, blending, and the evolution of cultural similarities and differences among human populations. *Evol. Hum. Behav.* **27**, 169–184 (2006).
7. Morrison, D. A. Are phylogenetic patterns the same in anthropology and biology? *bioRxiv* (2014).
8. Lemoine, F., Blassel, L., Voznica, J. & Gascuel, O. COVID-Align: Accurate online alignment of hCoV-19 genomes using a profile HMM. *Bioinformatics* **37**, 1761–1762 (2021).
9. O’Toole, Á. *et al.* Assignment of epidemiological lineages in an emerging pandemic using the pangolin tool. *Virus Evol.* **7**, veab064 (2021).
10. Attwood, S. W., Hill, S. C., Aanensen, D. M., Connor, T. R. & Pybus, O. G. Phylogenetic and phylodynamic approaches to understanding and combating the early SARS-CoV-pandemic. *Nat. Rev. Genet.* **23**, 547–562 (2022).
11. Sanderson, T. Taxonium, a web-based tool for exploring large phylogenetic trees. *eLife* **11** (2022).
12. Turakhia, Y. *et al.* Pandemic-scale phylogenomics reveals the SARS-CoV-2 recombination landscape. *Nature* **609**, 994–997 (2022).
13. Voznica, J. *et al.* Deep learning from phylogenies to uncover the epidemiological dynamics of outbreaks. *Nat. Commun.* **13**, 1–14 (2022).
14. De Maio, N. *et al.* Maximum likelihood pandemic-scale phylogenetics. *Nature Genetics*, 1–7 (2023).
15. Sanderson, M. J. & Shaffer, H. B. Troubleshooting molecular phylogenetic analyses. *Annu. Rev. Ecol. Syst.* **33**, 49–72 (2002).
16. Yang, Z. *Computational molecular evolution* (OUP Oxford, 2006).
17. Yang, Z. & Rannala, B. Molecular phylogenetics: principles and practice. *Nat. Rev. Genet.* **13**, 303–314 (2012).
18. Lee, M. S. & Palci, A. Morphological phylogenetics in the genomic age. *Curr. Biol.* **25**, R922–R929 (2015).
19. Morlon, H., Parsons, T. L. & Plotkin, J. B. Reconciling molecular phylogenies with the fossil record. *Proc. Natl. Acad. Sci. U.S.A.* **108**, 16327–16332 (2011).
20. Arato, J. & Fitch, W. T. Phylogenetic signal in the vocalizations of vocal learning and vocal non-learning birds. *Philos. Trans. R. Soc. Lond. B Biol. Sci.* **376**, 20200241 (2021).
21. Bromham, L. & Penny, D. The modern molecular clock. *Nat. Rev. Genet.* **4**, 216–224 (2003).
22. Dos Reis, M., Donoghue, P. C. & Yang, Z. Bayesian molecular clock dating of species divergences in the genomics era. *Nat. Rev. Genet.* **17**, 71–80 (2016).
23. Zuckerkandl, E. Molecular disease, evolution, and genetic heterogeneity. *Horiz. Biochem. Biophys.*, 189–225 (1962).
24. Foulds, L. R. & Graham, R. L. The Steiner problem in phylogeny is NP-complete. *Adv. Appl. Math.* **3**, 43–49 (1982).
25. Day, W. H., Johnson, D. S. & Sankoff, D. The computational complexity of inferring rooted phylogenies by parsimony. *Math. Biosci.* **81**, 33–42 (1986).

26. Roch, S. A short proof that phylogenetic tree reconstruction by maximum likelihood is hard. *IEEE/ACM Trans. Comput. Biol. Bioinform.* **3**, 92–94 (2006).
27. Catanzaro, D., Labbé, M., Pesenti, R. & Salazar-González, J.-J. The Balanced Minimum Evolution Problem. *INFORMS J. Comput.* **24**, 276–294 (2012).
28. Hendy & Penny, D. Branch and bound algorithms to determine minimal evolutionary trees. *Math. Biosci.* **59**, 277–290 (1982).
29. Huelsenbeck, J. P. & Ronquist, F. MRBAYES: Bayesian inference of phylogenetic trees. *Bioinformatics* **17**, 754–755 (2001).
30. Wilgenbusch, J. C. & Swofford, D. Inferring evolutionary trees with PAUP. *Curr. Protoc. Bioinformatics*, 6.4.1–6.4.28 (2003).
31. Drummond, A. J. & Rambaut, A. BEAST: Bayesian evolutionary analysis by sampling trees. *BMC Evol. Biol.* **7**, 214 (2007).
32. Yang, Z. PAML 4: phylogenetic analysis by maximum likelihood. *Mol. Biol. Evol.* **24**, 1586–1591 (2007).
33. Stamatakis, A. RAXML version 8: a tool for phylogenetic analysis and post-analysis of large phylogenies. *Bioinformatics* **30**, 1312–1313 (2014).
34. Kozlov, A. M., Darriba, D., Flouri, T., Morel, B. & Stamatakis, A. RAXML-NG: a fast, scalable and user-friendly tool for maximum likelihood phylogenetic inference. *Bioinformatics* **35**, 4453–4455 (2019).
35. Lefort, V., Desper, R. & Gascuel, O. FastME 2.0: a comprehensive, accurate, and fast distance-based phylogeny inference program. *Mol. Biol. Evol.* **32**, 2798–2800 (2015).
36. Nguyen, L.-T., Schmidt, H. A., Von Haeseler, A. & Minh, B. Q. IQ-TREE: a fast and effective stochastic algorithm for estimating maximum-likelihood phylogenies. *Mol. Biol. Evol.* **32**, 268–274 (2015).
37. Minh, B. Q. *et al.* IQ-TREE 2: new models and efficient methods for phylogenetic inference in the genomic era. *Mol. Biol. Evol.* **37**, 1530–1534 (2020).
38. Park, H. J., Sul, S.-J. & Williams, T. L. Large-scale analysis of phylogenetic search behavior. *Adv. Exp. Med. Biol.* **680**, 35–42 (2010).
39. Sanderson, M. J., McMahon, M. M. & Steel, M. Terraces in phylogenetic tree space. *Science* **333**, 448–450 (2011).
40. Rokas, A., Williams, B. L., King, N. & Carroll, S. B. Genome-scale approaches to resolving incongruence in molecular phylogenies. *Nature* **425**, 798–804 (2003).
41. De Queiroz, A. & Gatesy, J. The supermatrix approach to systematics. *Trends Ecol. Evol.* **22**, 34–41 (2007).
42. St. John, K. The Shape of Phylogenetic Treespace. *Syst. Biol.* **66**, e83–e94 (2017).
43. Dinh, V., Bilge, A., Zhang, C. & Matsen IV, F. A. *Probabilistic Path Hamiltonian Monte Carlo* in *ICML* **70** (PMLR, 2017), 1009–1018.
44. Billera, L. J., Holmes, S. P. & Vogtmann, K. Geometry of the Space of Phylogenetic Trees. *Adv. Appl. Math.* **27**, 733–767 (2001).
45. Zhang, C. & Matsen IV, F. A. *Variational Bayesian phylogenetic inference* in *ICLR* (2018).
46. Nesterenko, L., Boussau, B. & Jacob, L. Phyloformer: towards fast and accurate phylogeny estimation with self-attention networks. *bioRxiv*, 2022–06 (2022).
47. Ayres, D. L. *et al.* BEAGLE: an application programming interface and high-performance computing library for statistical phylogenetics. *Syst. Biol.* **61**, 170–173 (2012).
48. Pauplin, Y. Direct calculation of a tree length using a distance matrix. *J. Mol. Evol.* **51**, 41–47 (2000).
49. Desper, R. & Gascuel, O. Fast and accurate phylogeny reconstruction algorithms based on the minimum-evolution principle. *J. Comput. Biol.* **9**, 687–705 (2002).
50. Kidd, K. K. & Sgaramella-Zonta, L. A. Phylogenetic analysis: concepts and methods. *Am. J. Hum. Genet.* **23**, 235–252 (1971).
51. Roch, S. Toward extracting all phylogenetic information from matrices of evolutionary distances. *Science* **327**, 1376–1379 (2010).
52. Rzhetsky, A. & Nei, M. A simple method for estimating and testing minimum-evolution trees. *Mol. Biol. Evol.* **9**, 945–967 (1992).
53. Desper, R. & Gascuel, O. Theoretical foundation of the balanced minimum evolution method of phylogenetic inference and its relationship to weighted least-squares tree fitting. *Mol. Biol. Evol.* **21**, 587–598 (2004).
54. Kuhner, M. K. & Felsenstein, J. A simulation comparison of phylogeny algorithms under equal and unequal evolutionary rates. *Mol. Biol. Evol.* **11**, 459–468 (1994).
55. Kumar, S. & Gadagkar, S. R. Efficiency of the neighbor-joining method in reconstructing deep and shallow evolutionary relationships in large phylogenies. *J. Mol. Evol.* **51**, 544 (2000).
56. Gascuel, O. & Steel, M. Neighbor-joining revealed. *Mol. Biol. Evol.* **23**, 1997–2000 (2006).
57. Penn, M. J., Scheidwasser, N., Khurana, M., Donnelly, C. A. & Bhatt, S. *Phylo2Vec: A vector representation of binary trees* in *2023 ICLR First Workshop on Machine Learning and Global Health* (2023).
58. Felsenstein, J. The Number of Evolutionary Trees. *Syst. Biol.* **27**, 27–33 (1978).
59. Kingma, D. P. & Ba, J. *Adam: A Method for Stochastic Optimization* in *ICLR* (2015).
60. Loshchilov, I. & Hutter, F. *Decoupled Weight Decay Regularization* in *ICLR* (2019).
61. Shazeer, N. & Stern, M. *Adafactor: Adaptive learning rates with sublinear memory cost* in *ICML* (2018), 4596–4604.
62. Chen, H.-C. & Wang, Y.-L. An efficient algorithm for generating Prüfer codes from labelled trees. *Theory Comput. Syst.* **33**, 97–105 (2000).
63. Diaconis, P. W. & Holmes, S. P. Matchings and phylogenetic trees. *Proc. Natl. Acad. Sci. U.S.A.* **95**, 14600–14602 (1998).
64. Fitch, W. M. & Margoliash, E. Construction of phylogenetic trees. *Science* **155**, 279–284 (1967).
65. Felsenstein, J. Statistical inference of phylogenies. *J R Stat Soc Ser A* **146**, 246–262 (1983).
66. Saitou, N. & Nei, M. The neighbor-joining method: a new method for reconstructing phylogenetic trees. *Mol. Biol. Evol.* **4**, 406–425 (1987).
67. Felsenstein, J. Cases in which Parsimony or Compatibility Methods will be Positively Misleading. *Syst. Biol.* **27**, 401–410 (1978).
68. Semple, C. & Steel, M. Cyclic permutations and evolutionary trees. *Adv. Appl. Math.* **32**, 669–680 (2004).

69. Atteson, K. The Performance of Neighbor-Joining Methods of Phylogenetic Reconstruction. *Algorithmica* **25**, 251–278 (1999).
70. Mihaescu, R., Levy, D. & Pachter, L. Why neighbor-joining works. *Algorithmica* **54**, 1–24 (2009).
71. Mihaescu, R. & Pachter, L. Combinatorics of least-squares trees. *Proc. Natl. Acad. Sci. U.S.A.* **105**, 13206–13211 (2008).
72. To, T.-H., Jung, M., Lycett, S. & Gascuel, O. Fast Dating Using Least-Squares Criteria and Algorithms. *Syst. Biol.* **65**, 82–97 (2016).
73. Bradbury, J. *et al.* JAX: composable transformations of Python+NumPy programs version 0.3.13. 2018. <http://github.com/google/jax>.
74. Irisarri, I. *et al.* Phylotranscriptomic consolidation of the jawed vertebrate timetree. *Nat. Ecol. Evol.* **1**, 1370–1378 (2017).
75. Hedges, S. B., Moberg, K. D. & Maxson, L. R. Tetrapod phylogeny inferred from 18S and 28S ribosomal RNA sequences and a review of the evidence for amniote relationships. *Mol. Biol. Evol.* **7**, 607–633 (1990).
76. Garey, J. R., Near, T. J., Nonnemacher, M. R. & Nadler, S. A. Molecular evidence for Acanthocephala as a subtaxon of Rotifera. *J. Mol. Evol.* **43**, 287–292 (1996).
77. Yang, Z. & Yoder, A. D. Comparison of likelihood and Bayesian methods for estimating divergence times using multiple gene loci and calibration points, with application to a radiation of cute-looking mouse lemur species. *Syst. Biol.* **52**, 705–716 (2003).
78. Henk, D. A., Weir, A. & Blackwell, M. Laboulbeniopsis termitarius, an ectoparasite of termites newly recognized as a member of the Laboulbeniomyces. *Mycologia* **95**, 561–564 (2003).
79. Brower, A. V. Phylogenetic relationships among the Nymphalidae (Lepidoptera) inferred from partial sequences of the wingless gene. *Proc. R. Soc. Lond. B Biol. Sci.* **267**, 1201–1211 (2000).
80. Lakner, C., Van Der Mark, P., Huelsenbeck, J. P., Larget, B. & Ronquist, F. Efficiency of Markov chain Monte Carlo tree proposals in Bayesian phylogenetics. *Syst. Biol.* **57**, 86–103 (2008).
81. Zhang, N. & Blackwell, M. Molecular phylogeny of dogwood anthracnose fungus (*Discula destructiva*) and the Diaporthales. *Mycologia* **93**, 355–365 (2001).
82. Yoder, A. D. & Yang, Z. Divergence dates for Malagasy lemurs estimated from multiple gene loci: geological and evolutionary context. *Mol. Ecol.* **13**, 757–773 (2004).
83. Rossman, A. Y., McKemy, J. M., Pardo-Schultheiss, R. A. & Schroers, H.-J. Molecular studies of the Bionectriaceae using large subunit rDNA sequences. *Mycologia* **93**, 100–110 (2001).
84. Ingram, A. L. & Doyle, J. J. Is *Eragrostis* (Poaceae) monophyletic? Insights from nuclear and plastid sequence data. *Syst. Bot.* **29**, 545–552 (2004).
85. Suh, S.-O. & Blackwell, M. Molecular phylogeny of the cleistothecial fungi placed in Cephalothecaceae and Pseudeurotiaceae. *Mycologia* **91**, 836–848 (1999).
86. Kroken, S. & Taylor, J. W. Phylogenetic species, reproductive mode, and specificity of the green alga *Trebouxia* forming lichens with the fungal genus *Letharia*. *Bryologist*, 645–660 (2000).
87. Song, S., Liu, L., Edwards, S. V. & Wu, S. Resolving conflict in eutherian mammal phylogeny using phylogenomics and the multispecies coalescent model. *Proc. Natl. Acad. Sci. U.S.A.* **109**, 14942–14947 (2012).
88. Hasegawa, M. & Kishino, H. Confidence limits of the maximum-likelihood estimate of the hominoid three from mitochondrial-DNA sequences. *Evolution* **43**, 672–677 (1989).
89. Paradis, E., Claude, J. & Strimmer, K. APE: analyses of phylogenetics and evolution in R language. *Bioinformatics* **20**, 289–290 (2004).
90. Whidden, C. & Matsen 4th, F. A. Quantifying MCMC exploration of phylogenetic tree space. *Syst. Biol.* **64**, 472–491 (2015).
91. Felsenstein, J. Evolutionary trees from DNA sequences: a maximum likelihood approach. *J. Mol. Evol.* **17**, 368–376 (1981).
92. Le, S. Q. & Gascuel, O. An improved general amino acid replacement matrix. *Mol. Biol. Evol.* **25**, 1307–1320 (2008).
93. Jukes, T. H., Cantor, C. R., *et al.* Evolution of protein molecules. *Mamm. Protein Metab.* **3**, 21–132 (1969).
94. Tamura, K. & Nei, M. Estimation of the number of nucleotide substitutions in the control region of mitochondrial DNA in humans and chimpanzees. *Mol. Biol. Evol.* **10**, 512–526 (1993).
95. Tieleman, T. & Hinton, G. *Lecture 6e - rmsprop: Divide the gradient by a running average of its recent magnitude* Coursera: Neural networks for machine learning. Slides. 2012. [https://www.cs.toronto.edu/~tijmen/csc321/slides/lecture\\_slides\\_lec6.pdf](https://www.cs.toronto.edu/~tijmen/csc321/slides/lecture_slides_lec6.pdf).
96. Gascuel, O. BIONJ: an improved version of the NJ algorithm based on a simple model of sequence data. *Mol. Biol. Evol.* **14**, 685–695 (1997).
97. Saitou, N. & Nei, M. The neighbor-joining method: a new method for reconstructing phylogenetic trees. *Mol. Biol. Evol.* **4**, 406–425 (1987).
98. Babuschkin, I. *et al.* The DeepMind JAX Ecosystem 2020. <http://github.com/deepmind>.
99. Gautier, L., Krassowski, M., *et al.* rpy2: Python interface to the R language 2021. <https://github.com/rpy2/rpy2>.
100. Huerta-Cepas, J., Serra, F. & Bork, P. ETE 3: reconstruction, analysis, and visualization of phylogenomic data. *Mol. Biol. Evol.* **33**, 1635–1638 (2016).
101. Hagberg, A. A., Schult, D. A. & Swart, P. J. *Proc. SciPy* in (2008), 11–15.
102. Zhang, C., Rabiee, M., Sayyari, E. & Mirarab, S. ASTRAL-III: polynomial time species tree reconstruction from partially resolved gene trees. *BMC Bioinform.* **19**, 15–30 (2018).
103. Robinson, D. F. & Foulds, L. R. Comparison of phylogenetic trees. *Math. Biosci.* **53**, 131–147 (1981).
104. Betancourt, M. A conceptual introduction to Hamiltonian Monte Carlo. *arXiv preprint arXiv:1701.02434* (2017).
105. Huelsenbeck, J. P., Bollback, J. P. & Levine, A. M. Inferring the root of a phylogenetic tree. *Syst. Biol.* **51**, 32–43 (2002).
106. Tria, F. D. K., Landan, G. & Dagan, T. Phylogenetic rooting using minimal ancestor deviation. *Nat. Ecol. Evol.* **1**, 193 (2017).
107. Naser-Khdour, S., Quang Minh, B. & Lanfear, R. Assessing Confidence in Root Placement on Phylogenies: An

- Empirical Study Using Nonreversible Models for Mammals. *Syst. Biol.* **71**, 959–972 (2022).
108. Vankan, M., Ho, S. Y. W. & Duchêne, D. A. Evolutionary Rate Variation among Lineages in Gene Trees has a Negative Impact on Species-Tree Inference. *Syst. Biol.* **71**, 490–500 (2022).
  109. Suchard, M. A., Kitchen, C. M. R., Sinsheimer, J. S. & Weiss, R. E. Hierarchical phylogenetic models for analyzing multipartite sequence data. *Syst. Biol.* **52**, 649–664 (2003).
  110. Duchêne, S. *et al.* Cross-validation to select Bayesian hierarchical models in phylogenetics. *BMC Evol. Biol.* **16**, 115 (2016).

Zoonotic Infections, a partnership between the UK Health Security Agency, University of Liverpool, University of Oxford and Liverpool School of Tropical Medicine (grant code NIHR200907). D.A.D. is funded by a European Research Council Marie Skłodowska-Curie fellowship (H2020-MSCA-IF-2019-883832). M.P. was funded by a DTP Studentship from the Engineering and Physical Sciences Research (EPSRC)

## Author contributions

S.B and M.J.P conceived of the study. S.B and C.A.D supervised. S.B, N.S, M.J.P and D.A.D designed the study. S.B and N.S performed optimisation runs. S.B, M.J.P, N.S and D.A.D performed analysis. All authors contributed to writing the original draft. M.J.P and J.P drafted the appendix.

## Competing interests

The authors declare no competing interests.

## Funding

S.B. and C.A.D acknowledges support from the MRC Centre for Global Infectious Disease Analysis (MR/R015600/1), jointly funded by the UK Medical Research Council (MRC) and the UK Foreign, Commonwealth & Development Office (FCDO), under the MRC/FCDO Concordat agreement, and also part of the EDCTP2 programme supported by the European Union. SB is funded by the National Institute for Health Research (NIHR) Health Protection Research Unit in Modelling and Health Economics, a partnership between the UK Health Security Agency, Imperial College London and LSHTM (grant code NIHR200908). Disclaimer: “The views expressed are those of the author(s) and not necessarily those of the NIHR, UK Health Security Agency or the Department of Health and Social Care.” S.B. acknowledges support from the Novo Nordisk Foundation via The Novo Nordisk Young Investigator Award (NNF20OC0059309). S.B. acknowledges support from the Danish National Research Foundation via a chair grant which also supports N.S. S.B. acknowledges support from The Eric and Wendy Schmidt Fund For Strategic Innovation via the Schmidt Polymath Award (G-22-63345). S.B and N.S acknowledge the Pioneer Centre for AI, DNRF grant number P1 as affiliate researchers. C.A.D receives support from the NIHR HPRU in Emerging and



## Appendix

### A. Background

**Binary trees.** A binary tree is a tree where every node has degree 1 or 3, with the possible exception of a single node of degree 2. The nodes of degree 1 are called *leaves*, the nodes of degree 3 are called *internal nodes* and the node of degree 2, if it exists, is called the *root*. A tree with a root is called *rooted*; otherwise, it is called *unrooted*.

In a rooted tree, we define the *generation* of a node to be the path length between that node and the root. We define the *children* of a node  $x$  to be any nodes sharing an edge with  $x$  with generation one higher than the generation of  $x$ . We define the *parent* of a node to be any nodes sharing an edge with  $x$  with generation one lower than  $x$ .

**Phylogenetic inference.** We consider a tree with  $n$  taxa with names  $N_0, \dots, N_{n-1}$ . Initially, we suppose that the leaf node corresponding to the taxon with name  $N_i$  has label  $i$ . A phylogenetic tree is a representation of the evolutionary history of these taxa. It is a binary tree where each of the leaves correspond to a taxon. Depending on the problem under consideration, it may be either rooted or unrooted.

Introduced in [57], Phylo2Vec provides a bijective mapping between the space of rooted phylogenetic trees with  $n$  taxa and integer-valued vectors  $v$  satisfying

$$v_0 = 0 \quad \text{and} \quad v_m \in \{0, 1, \dots, 2(m-1)\} \quad \forall m \in \{1, \dots, n-1\} \quad (3)$$

Hence, we are able to refer uniquely to a rooted tree by its vector representation  $v$ . As discussed in [57], for a given unrooted tree, there are  $2n-1$  vectors which, when the root of the corresponding tree is removed, result in this unrooted tree.

In balanced minimum evolution (BME), traditionally applied to unrooted trees (though we justify its use for rooted trees in the following section), we are provided with a matrix  $D$  giving the distance between each pair of taxa. For a given tree, we also calculate the matrix  $e$ , giving the (unweighted) path length between the leaf nodes corresponding to each pair of taxa. The objective value of this tree is then  $f(v) = \sum_{ij} D_{ij} 2^{-e_{ij}}$ , and the aim of our optimisation algorithm is to find the tree which minimises  $f$ .

### B. BME for rooted trees

**A rooted tree via a distant ancestor.** The application of BME is almost always restricted to unrooted trees [68]. However, we present below a justification for its use in rooted tree space also. Suppose that we have a set of  $n$  taxa labelled  $\{0, 1, \dots, n-1\}$ . We introduce a new taxon, labelled  $n$ , which is considered a very distant root. Under the (almost always biologically reasonable) assumption that the root evolved long before the other taxa, this root will be approximately independent of all the other taxa. That is, we expect

$$D_{ni} = D^* + O(\epsilon) \quad \forall i \neq n \quad (4)$$

for  $\epsilon \ll 1$ , where  $\epsilon$  includes both the error from the root not being completely independent of the taxa, and also the aleatoric error in the distance between two independent species. If our distance matrix were based on genetic sequence data, we would need the sequence to be sufficiently long to ensure this aleatoric error was small. This result holds regardless of the distances between the other taxa. Hence, note that, for any unrooted tree with internode path lengths  $e_{ij}$ ,

$$\sum_{i,j} D_{ij} 2^{-e_{ij}} = \sum_j D_{nj} 2^{-e_{nj}} + \sum_i D_{in} 2^{-e_{in}} + \sum_{i,j < n} D_{ij} 2^{-e_{ij}} \quad (5)$$

$$= \sum_j (D^* + O(\epsilon)) 2^{-e_{nj}} + \sum_i (D^* + O(\epsilon)) 2^{-e_{in}} + \sum_{i,j < n} D_{ij} 2^{-e_{ij}} \quad (6)$$

We can make progress with this sum by noting the Kraft Equality, found throughout the literature [27]

$$\sum_j 2^{-e_{nj}} = \frac{1}{2} \quad (7)$$

This means that

$$\sum_{i,j} D_{ij} 2^{-e_{ij}} = \sum_{i,j < n} D_{ij} 2^{-e_{ij}} + \frac{D^*}{2} + O(\epsilon) \quad (8)$$

Moreover, if there exists some small  $\delta$  such that

$$|D_{na} - D^*| \leq \delta \quad \forall a \neq n \quad (9)$$

then a similar argument shows

$$\left| \sum_{i,j} D_{ij} 2^{-e_{ij}} - \sum_{i,j < n} D_{ij} 2^{-e_{ij}} - \frac{D^*}{2} \right| \leq \frac{\delta}{2} \quad (10)$$

Thus, provided that there is a unique optimal tree  $\mathcal{T}$  minimising  $\sum_{i,j} D_{ij} 2^{-e_{ij}}$ , the finiteness of tree space ensures that, for sufficiently small  $\delta$ ,  $\mathcal{T}$  is also the unique minimiser of  $\sum_{i,j < n} D_{ij} 2^{-e_{ij}}$ .

Hence, assuming the existence of a sufficiently distant ancestor (and assuming sufficiently small aleatoric error) the optimal unrooted tree for the  $n + 1$  taxa can be found by finding the optimal *rooted* tree for  $n$  taxa with the objective function  $\sum_{i,j < n} D_{ij} 2^{-e_{ij}}$  - that is, the standard BME objective applied to rooted trees with  $n$  taxa. This means that the BME objective function can be applied to rooted trees, even though the addition of the root means that it is no longer equal to the tree length. Moreover, applying it in this way provides a way, in theory, to find the root of a set of taxa as this root node is, in our  $n + 1$  taxa tree, joined to the distant ancestor which we know is the true outgroup. However, as discussed in the following sections, this root may be incorrect when different branches on the tree had different evolutionary rates.

**The rooting problem.** Suppose we have an unrooted tree  $\mathcal{T}$  and that we want to find the optimal rooting for this tree - that is, the edge in the tree such that placing the root on this edge minimizes the BME objective.

Choose an edge,  $b$  on which to place the root. We define a function  $X_b$  such that  $X_b(A, B)$  is 1 if  $b$  is on the path between nodes  $A$  and  $B$ . Adding a root to edge  $b$  changes the objective function by halving the weight assigned to each  $D_{AB}$  such that  $X_b(A, B) = 1$  as the path length between these nodes will increase by 1. Thus, using  $f_r$  to denote the rooted objective and  $f_u$  to denote the unrooted objective,

$$f_r = f_u - \frac{1}{2} \sum_{X_b(A,B)=1} D_{AB} 2^{-e_{AB}} \quad (11)$$

where the  $e_{AB}$  are the path lengths in the original, unrooted tree and both  $A$  and  $B$  are allowed to vary in the sum. Hence, for a fixed unrooted tree topology, the optimal rooting will solve

$$\max_b \left\{ \sum_{X_b(A,B)=1} D_{AB} 2^{-e_{AB}} \right\} \quad (12)$$

**Reformulating the rooting problem.** To make progress in interpreting the solution to the rooting problem (12), we use the common BME assumption that in the optimal unrooted tree  $\mathcal{T}$ , there exist edge weights such that  $D_{AB}$  is the length between nodes  $A$  and  $B$  in the tree  $\mathcal{T}$  (practically, BME arises from a least squares approximation to these lengths).

**Claim:** If  $D_{Ar}$  is the distance between node  $A$  and the root, and  $g_A$  is the path length (i.e. the generation of node  $A$ ), then

$$\sum_{X_b(A,B)=1} D_{AB} 2^{-e_{AB}} = 2 \sum_A 2^{-g_A} D_{Ar} \quad (13)$$

**Proof:** Again, the  $e_{AB}$  terms refer to the path lengths in the original unrooted tree. (13) can be proved by induction on the number of leaf nodes,  $n$ . For  $n = 2$ , the root must be placed on the edge connecting nodes 0 and 1 and  $e_{01} = 1$ . Then

$$\sum_{X_b(A,B)=1} D_{AB} 2^{-e_{AB}} = \frac{1}{2} (D_{01} + D_{10}) = \left( 2^{1-1} D_{0r} + 2^{1-1} D_{1r} \right) \quad (14)$$

as required, noting that  $D_{0r} + D_{1r} = D_{01}$ . Suppose that our claim holds for  $n = k$  and consider a tree with  $n = k + 1$ . Choose a pair of sibling leaf nodes (i.e. leaf nodes joined to the same internal node)  $y$  and  $z$  such that the root is not on an

edge joining one of these nodes to the tree (this must exist as, for  $n > 2$ , there are at least two pairs of sibling leaf nodes). Suppose that  $y$  and  $z$  are connected to the internal node  $w$ . Now, note that the contribution to the objective of node  $y$  is

$$2 \sum_{B: X_b(y, B)=1} D_{yB} 2^{-e_{yB}} = 2 \sum_{B: X_b(w, B)=1} (D_{wB} + D_{wy}) 2^{-e_{yB}} \quad (15)$$

$$= 2 \sum_{B: X_b(w, B)=1} D_{wB} 2^{-e_{yB}} + 2D_{wy} \sum_{B: X_b(w, B)=1} 2^{-e_{yB}} \quad (16)$$

$$= \sum_{B: X_b(w, B)=1} D_{wB} 2^{-e_{wB}} + 2D_{wy} \sum_{B: X_b(w, B)=1} 2^{-e_{yB}} \quad (17)$$

where the factor of 2 comes from the fact that both  $(y, B)$  and  $(B, y)$  must be considered. The final term in this equation can be simplified. Consider the subtree whose leaves are the root and all nodes such that  $X_b(w, B) = 1$ . Then, by the Kraft Equality on this subtree

$$\sum_{B: X_b(w, B)=1} 2^{-g_B} = \frac{1}{2} \quad (18)$$

as  $g_B$  gives the distance between the root and node  $B$ . Moreover, as  $e_{yB} = g_y + g_B - 1$  (where the  $-1$  accounts for the fact that  $\mathcal{T}$  is unrooted)

$$\sum_{B: X_b(w, B)=1} 2^{-e_{yB}} = 2^{1-g_y} \sum_{B: X_b(w, B)=1} 2^{-g_B} = 2^{-g_y} \quad (19)$$

Thus, (17) becomes

$$2 \sum_{X_b(y, B)=1} D_{yB} 2^{-e_{yB}} = \sum_{B: X_b(w, B)=1} D_{wB} 2^{-e_{wB}} + 2D_{wy} 2^{-g_y} \quad (20)$$

Thus, the change to  $\sum_{X_b(A, B)=1} D_{AB} 2^{-e_{AB}}$  caused by adding nodes  $y$  and  $z$  from the tree is to subtract

$$2 \sum_{X_b(w, B)=1} D_{wB} 2^{-e_{wB}} \quad (21)$$

(as node  $w$  is no longer a leaf node) and to add the contributions from nodes  $y$  and  $z$

$$2 \left( \sum_{B: X_b(y, B)=1} D_{yB} 2^{-e_{yB}} + \sum_{B: X_b(z, B)=1} D_{zB} 2^{-e_{zB}} \right) = \sum_{X_b(w, B)=1} D_{wB} 2^{-e_{wB}} + 2D_{wy} 2^{-g_y} + \sum_{X_b(w, B)=1} D_{wB} 2^{-e_{wB}} + 2D_{wz} 2^{-g_z} \quad (22)$$

There is no  $(y, z)$  term to consider as  $X_b(y, z) = 0$ . Note that the  $\sum_{X_b(w, B)=1} D_{wB} 2^{-e_{wB}}$  terms cancel. Define  $\mathcal{T}'$  to be the tree when node  $y$  and  $z$  are removed so, as it now has  $k$  leaf nodes, the inductive hypothesis can be used to show

$$\sum_{A, B \in \mathcal{T}: X_b(A, B)=1} D_{AB} 2^{-e_{AB}} = \sum_{A', B' \in \mathcal{T}': X'_b(A', B')=1} D_{A'B'} 2^{-e'_{A'B'}} + 2D_{wy} 2^{-g_y} + 2D_{wz} 2^{-g_z} \quad (23)$$

$$= 2 \sum_{A' \in \mathcal{T}'} 2^{-g'_{A'}} D_{A'r'} + 2D_{wy} 2^{-g_y} + 2D_{wz} 2^{-g_z} \quad (24)$$

$$= 2 \sum_{A' \in \mathcal{T}'/\{w\}} 2^{-g'_{A'}} D_{A'r'} + 2D_{wr} 2^{-g_w} + 2D_{wy} 2^{-g_y} + 2D_{wz} 2^{-g_z} \quad (25)$$

where dashes are used to denote quantities in  $\mathcal{T}'$ . Note that

$$\sum_{A' \in \mathcal{T}'/\{w\}} 2^{-g'_{A'}} D_{A'r'} = \sum_{A \in \mathcal{T}/\{y, z\}} 2^{-g_A} D_{Ar} \quad (26)$$

as only the nodes  $w, y$  and  $z$  are affected by changing from  $\mathcal{T}$  to  $\mathcal{T}'$ . Moreover, note that

$$2^{-g_w} = 2^{-g_y} + 2^{-g_z} \quad (27)$$

as  $g_w = g_y - 1 = g_z - 1$ , and, as the distances are additive,

$$D_{wy} + D_{wr} = D_{yr} \quad \text{and} \quad D_{wz} + D_{wr} = D_{zr} \quad (28)$$

Hence

$$2D_{wy}2^{-g_y} + 2D_{wz}2^{-g_z} + 2D_{wr}2^{-g_w} = 2D_{wy}2^{-g_y} + 2D_{wz}2^{-g_z} + 2D_{wr}(2^{-g_y} + 2^{-g_z}) \quad (29)$$

$$= 2(D_{wy} + D_{wr})2^{-g_y} + 2(D_{wz} + D_{wr})2^{-g_z} \quad (30)$$

$$= 2D_{yr}2^{-g_y} + 2D_{zr}2^{-g_z} \quad (31)$$

Thus,

$$\sum_{X_b(A,B)=1} D_{AB}2^{-e_{AB}} = \sum_A 2^{-g_A} D_{Ar} \quad (32)$$

and hence the claim holds by induction as required.

**Rooting in ultrametric trees.** Under the assumption that distances are additive (that is, one can find the distance between node  $A$  and  $B$  by summing the lengths of the edges on the path from  $A$  to  $B$ ) we make the further assumption that (after scaling) the length of each edge is approximately equal to the amount of time associated with the evolution that occurred on this edge. We use the additional, biologically-motivated assumption that the leaf taxa are being observed at the same point in time. This means that the length in time from the root to each leaf in the tree is the same.

We can then estimate the true length of time from the root to the leaves (i.e. the length of the evolutionary process represented by the tree) from the following simple heuristic. Given two leaf nodes that share a parent, define  $d_1$  and  $d_2$  to be the length of the edge between each child and its parent. We then approximate the true time between the children's divergence and the current time as  $\frac{d_1+d_2}{2}$ . Moreover, if their parent was at a distance  $d_3$  from its parent, we remove these children from the tree and redefine the edge length between their parent and its parent as  $d_3 + \frac{d_1+d_2}{2}$ .

We can continue this process inductively by continually choosing a pair of sibling leaf nodes, removing them, and updating the distance between their parent and its parent. We stop the process once we have only two leaf nodes remaining, and, if they are distances  $d_{n-2}$  and  $d_{n-1}$  from the root, we approximate the overall length of the tree to be  $\mathcal{D} = \frac{d_{n-2}+d_{n-1}}{2}$ .

**Claim:**

$$\mathcal{D} = \sum_A 2^{-g_A} D_{Ar} \quad (33)$$

**Proof:** This can be proved through induction on the number of nodes. It clearly holds if there are only two nodes in the tree. Assume it holds whenever there are  $k$  nodes, and consider a tree with  $k + 1$  nodes. We process the first pair of leaf nodes,  $y$  and  $z$ , and assume that their associated distances to their parent,  $w$  are  $D_{wy}$  and  $D_{wz}$  and that the new tree created is  $\mathcal{T}'$  with distances  $D'$ . Then, we have, by our inductive hypothesis

$$\mathcal{D} = \sum_{A' \in \mathcal{T}'} 2^{-g'_{A'}} D'_{A'r'} \quad (34)$$

$$= \sum_{A' \in \mathcal{T}'/\{w\}} 2^{-g'_{A'}} D'_{A'r'} + 2^{-g'_w} D'_{wr'} \quad (35)$$

$$= \sum_{A \in \mathcal{T}/\{y,z\}} 2^{-g_A} D_{Ar} + 2^{-g_w} \left( D_{wr} + \frac{D_{wy} + D_{wz}}{2} \right) \quad (36)$$

$$= \sum_{A \in \mathcal{T}/\{y,z\}} 2^{-g_A} D_{Ar} + 2^{-g_w} \left( \frac{D_{yr} + D_{zr}}{2} \right) \quad (37)$$

$$= \sum_{A \in \mathcal{T}} 2^{-g_A} D_{Ar} \quad (38)$$

as required, where we have used the fact that  $D_{wr} + D_{wy} = D_{yr}$  and that  $2^{g_w} = 2 \times 2^{-g_y} = 2 \times 2^{-g_z}$ .

**Interpreting the rooting problem.** The previous work has shown that, given an ultrametric *unrooted* tree, the optimal rooting maximises a heuristic for the root-to-tip distance in the tree. Equivalently, the optimal rooting ensures that the root is estimated to be the maximal possible distance back in time.

This is not an immediately biologically plausible objective for the root. Indeed, the cornerstone of BME is that we want the tree of *minimum* length, and it hence seems counter-intuitive to require the root that is the *maximum* distance backwards in time (though, of course, the previous work has showed that this will create the minimum length tree).

However, our assumption of a distant ancestor means that the root of our tree must be the point that is furthest backwards in time. In particular, this means that the evolutionary direction needs to be away from the root. By setting our root such that the root-to-tip distance is maximised, we ensure that the root satisfies this constraint.

This property will not hold if the tree is not ultrametric. If taxa evolve at different rates at different times throughout the tree, then the root will be drawn towards taxa with high evolutionary rates. Thus, caution must be used when applying our rooted algorithm to such trees, although the unrooted algorithm will still give a correct unrooted tree. In this case, it may be best to find the optimal unrooted tree topology and then solve the rooting problem for this tree, rather than finding the optimal rooted tree, as this will reduce the skewing effect of the heterogeneity in evolutionary rates.

### C. Ordered Trees

**Definition.** A tree,  $v$ , is *ordered* if

$$v_0 = 0 \quad \text{and} \quad v_i < i \quad \forall i \quad (39)$$

As discussed in [57], ordered trees have a number of desirable properties, and are useful for creating efficient phylogenetic optimisation algorithms.

**A left-to-right construction algorithm for ordered trees.** Under the assumption that  $v$  is ordered, it is possible to construct the tree in  $\mathcal{O}(n)$  time by processing the nodes from left-to-right (that is, from the lowest-labelled node to the highest-labelled node). This is in contrast to the normal Phylo2Vec algorithm which runs from right-to-left. An example is shown in Fig. 1.

One can do this by labelling the edges joining each leaf node to the rest of the tree with the same label as the leaf node (that is edge  $i$  joins leaf  $i$  to the rest of the tree). Then, after initialising with nodes 0 and 1 joined to the root, if  $v_j = k$ , node  $j$  is added to the tree by adding a new internal node on edge  $k$  and joining the node  $j$  to this edge (so that this new internal node has children  $j$  and  $k$ ).

**Equivalence with Phylo2Vec.** To show that the left-to-right algorithm gives an equivalent tree, define  $\mathcal{T}$  to be the tree resulting from the standard Phylo2Vec algorithm and  $\mathcal{T}'$  to be the tree resulting from this new left-to-right algorithm. We proceed by induction on the number of nodes,  $n$ , noting that the case  $n = 2$  is trivial.

Suppose now that the algorithms are equivalent for  $n = m$ . Choose some ordered  $v$  of length  $m + 1$  (so that this corresponds to  $n = m + 1$ ) and consider processing the first node using the Phylo2Vec algorithm, so that (using the fact that  $v$  is ordered so that no nodes are skipped), node  $m$  merges with node  $v_m$ .

From this step, the Phylo2Vec algorithm proceeds as if there were  $n - 1$  nodes and the vector was  $\tilde{v} = (v_0, v_1, \dots, v_{m-1})$ . Define  $\tilde{\mathcal{T}}$  to be the tree given by  $\tilde{v}$ . Hence,  $\tilde{\mathcal{T}}$  can be created from  $\mathcal{T}$  by removing nodes  $v_m$  and  $m$  (and the edges connecting them to the tree) and relabelling their parent as  $v_m$ . Equivalently (by reversing this process),  $\mathcal{T}$  can be created from  $\tilde{\mathcal{T}}$  by adding a node to the edge joining leaf node  $v_m$  to the tree, and connecting node  $m$  to this edge.

Moreover, from the inductive hypothesis,  $\tilde{\mathcal{T}}$  can be constructed by using the left-to-right algorithm on  $\tilde{v}$ . As this algorithm processes  $v_m$  last, this means that after  $m$  nodes have been added to the tree by the left-to-right algorithm applied to  $v$ , the current tree is given by  $\tilde{\mathcal{T}}$ .

The final step of the left-to-right algorithm applied to  $v$  is to add a node to the edge joining leaf node  $v_m$  to the tree, and to connect node  $m$  to this edge. As previously discussed, this creates the tree  $\mathcal{T}$  and hence,  $\mathcal{T} = \mathcal{T}'$  as required.

### D. A continuous objective function

**Setup.** There exists a natural continuous relaxation of the Phylo2Vec representation. Suppose that the Phylo2Vec vector of a tree is now a random variable  $\mathbf{V}$ . Consider a matrix  $W$  where

$$W_{ij} = \mathbb{P}(V_i = j) \quad (40)$$

so that  $W$  defines the distribution of  $\mathbf{V}$ . We ignore  $V_0$  in this construction as it is always equal to 0. For  $i > 0$ ,  $V_i < i$  and so  $W$  is a strictly lower-triangular matrix. To denote the dependence of  $\mathbf{V}$  on  $W$ , we shall write  $\mathbf{V} = \mathbf{V}(W)$ .



Given this distribution, one can then calculate the objective function as the expectation of the objective value of a tree drawn with distribution  $W$ . If  $f(\mathbf{v})$  is the objective function for a deterministic tree, then one can define

$$F(W) := \mathbb{E}[f(\mathbf{V}(W))] \quad (41)$$

If all the lower-triangular entries of  $W$  are non-zero, then  $\mathbf{V}$  can be any ordered tree with non-zero probability. Thus, a naive calculation of this expectation would need to consider the objective values of all  $(n-1)!$  ordered trees – a task that quickly becomes computationally infeasible for increasing  $n$ . However, we can exploit the Phylo2Vec construction to calculate this expectation in  $\mathcal{O}(n^3)$ , making this method feasible for trees with thousands of taxa.

**Finding edge lengths (rooted trees).** The objective function corresponding to the BME model relies on the quantities  $2^{-e_{ij}}$ , where  $e_{ij}$  is the path length between nodes  $i$  and  $j$  in the tree.

We can calculate an exact expectation,  $E_{ij} := \mathbb{E}(2^{-e_{ij}})$  for ordered trees by iteratively updating the  $E_{ij}$  throughout the left-to-right construction procedure. Adding node  $k$  to the tree increases the path length between nodes  $i$  and  $j$  by 1 if and only if  $V_k = i$  or  $V_k = j$ . As this condition is independent of other values of  $\mathbf{V}$ , using  $e_{ij}^k$  to be the path length after the  $k$  nodes  $\{0, \dots, k-1\}$  have been added, one can write

$$2^{-e_{ij}^{k+1}} = 2^{-(e_{ij}^k + \mathbb{I}\{V_k \in \{i, j\}\})} = 2^{-e_{ij}^k} \times 2^{-\mathbb{I}\{V_k \in \{i, j\}\}} \quad (42)$$

This is a product of independent random variables and so, defining  $E_{ij}^k := \mathbb{E}(2^{-e_{ij}^k})$  and noting that  $\mathbb{I}\{V_k \in \{i, j\}\}$  is a Bernoulli random variable with probability  $W_{ki} + W_{kj}$ , this equation becomes

$$E_{ij}^{k+1} = E_{ij}^k \left[ (1 - (W_{ki} + W_{kj})) + \frac{1}{2}(W_{ki} + W_{kj}) \right] = E_{ij}^k \left[ 1 - \frac{1}{2}(W_{ki} + W_{kj}) \right] \quad (43)$$

To close this iterative system, note that when node  $j$  is added to the tree, it will be a path length 2 from the leaf node  $V_j$  connecting the edge it is joined to. Moreover, the distance between node  $j$  and any other nodes  $x \neq V_j$  in the tree will be equal to one plus the distance between node  $x$  and node  $V_j$ . That is,

$$2^{-e_{ij}^{j+1}} = \begin{cases} 2^{-(1+e_{ix}^j)} & \text{if } V_j \neq i \\ \frac{1}{4} & \text{if } V_j = i \end{cases} \quad (44)$$

Thus, conditioning on the value of  $V_j$ ,

$$E_{ij}^{j+1} = \left[ \frac{1}{2} \sum_{x \neq i} E_{ix}^j W_{jx} \right] + \frac{1}{4} W_{ji} \quad (45)$$

Finally, by symmetry,  $E_{ji}^{j+1} = E_{ij}^{j+1}$ . Noting that  $E_{ij}^k$  is undefined (and unnecessary) for  $k < \max(i, j) + 1$ , as nodes  $i$  and  $j$  have not both been added to the tree, (43) and (45) hence form a closed system. This can be solved inductively, finding all  $E_{ij}^m$  terms for  $m = 2, 3, \dots, n$ .

To find the  $E_{ij}^m$  terms, there are  $\mathcal{O}(m)$  steps of  $\mathcal{O}(m)$  (finding the  $E_{m-1, j}^m$  terms) and  $\mathcal{O}(m^2)$  steps of  $\mathcal{O}(1)$  (finding the other  $E_{ij}^m$  terms). There are  $\mathcal{O}(n)$  values of  $m$  that need to be considered, and hence this system can be solved in  $\mathcal{O}(n^3)$  time.

Note that this method would not work in the case of unordered trees (in effect, this would be make it possible that new nodes are added to edges not connected to leaves). If node  $k$  were joined to some internal edge  $x$ , then  $e_{ij}$  would increase if edge  $x$  were on the path from  $i$  to  $j$ . However, this is clearly not independent of  $e_{ij}^k$ , and hence a similar iterative scheme cannot be derived.

**Objective function.** The objective function for BME is then

$$F(W) := \mathbb{E} \left[ \sum_{i \neq j} 2^{-e_{ij}^n} D_{ij} \right] = \sum_{i \neq j} D_{ij} E_{ij} \quad (46)$$

And the overall computation time remains  $\mathcal{O}(n^3)$  time (which is dominated by the calculation of the  $E_{ij}$  terms).

**Unrooted trees.** It may be preferable to calculate this objective for an unrooted tree. This can be done from the same construction, but where initially, nodes 0 and 1 are a distance 1 away from each other (rather than distance 2 in the rooted case). This, in effect, gives the edges that join the root a weight of  $\frac{1}{2}$  rather than 1, hence producing the correct path lengths. Thus, the only difference to the edges algorithm is that  $E_{01}^2 = \frac{1}{2}$  rather than  $\frac{1}{2}$ , and the rest of the algorithm proceeds identically (as, for example, adding a node to edge 0 still increases the distance between node 0 and all other nodes by 1).

## E. Properties of the continuous objective function

**Recovering the discrete objective function.** To recover the objective value of a deterministic tree  $\mathbf{v}$ , one can set

$$W_{ij} = \mathbb{I}\{v_i = j\} \quad (47)$$

This means that  $\mathbf{V}(W) = \mathbf{v}$  and hence  $f(\mathbf{v}) = F(W)$

**Discreteness of optima.** Noting that  $F(W)$  comes from an expectation, one can rewrite it as

$$F(W) = \sum_{\mathbf{v}} \mathbb{P}(\mathbf{V} = \mathbf{v}) f(\mathbf{v}) \quad (48)$$

$$= \sum_{\mathbf{v}} \left( \prod_{i=0}^n W_{i,v_i} \right) f(\mathbf{v}) \quad (49)$$

Noting that

$$\sum_{\mathbf{v}} \left( \prod_{i=1}^n W_{i-1,v_i} \right) = \sum_{\mathbf{v}} \mathbb{P}(\mathbf{V} = \mathbf{v}) = 1 \quad (50)$$

this means that the objective function is a weighted average of the objective values of all the deterministic trees. Thus, in particular, it is minimised when

$$\mathbb{P}(\mathbf{V} \in \{\mathbf{v} : f(\mathbf{v}) = \min_{\mathbf{s}} f(\mathbf{s})\}) = 1 \quad (51)$$

In general, the minimum of  $f$  is achieved at a unique tree,  $\mathbf{v}^*$  and hence,  $F(W)$  is minimised when

$$\mathbb{P}(\mathbf{V} = \mathbf{v}^*) = 1 \quad (52)$$

That is, it is minimised when  $\mathbf{V}$  is deterministically equal to the optimal tree. Thus, minimising  $F$  gives the same tree as minimising  $f$ .

**Finding  $\nabla F$ .** Note that, from (48),  $F$  is linear in each variable  $W_{ij}$  (when other variables are fixed). Thus, for any  $\epsilon > 0$ ,

$$(\nabla F)_{ab} = \frac{F(W + \epsilon X(a, b)) - F(W)}{\epsilon} \quad (53)$$

where  $X(a, b)$  is a matrix with  $(a, b)$  entry equal to 1 and all other entries equal to 0. This is exact for all  $\epsilon$  rather than approximate for small  $\epsilon$  because of the linearity. Similar calculations can be made for the Hessian (and indeed higher derivatives). Note that the matrix  $W + \epsilon X(a, b)$  lacks phylogenetic interpretability, but nevertheless can be assigned a value of  $F$  for finding the gradient.

**Single-step approximation.** One can approximate the optimal ordered tree after a single gradient step from a uniformly distributed tree.

To show this, consider the objective function as written in (49). That is,

$$F(W) = \sum_{\mathbf{v}} \left( \prod_{i=0}^n W_{i,v_i} \right) f(\mathbf{v}) \quad (54)$$

Note that

$$(\nabla F)_{ab} = \sum_{\mathbf{v}: v_a = b} \left( \prod_{i \neq a} W_{i,v_i} \right) f(\mathbf{v}) \quad (55)$$

As the distribution is uniform, the product  $\prod_{i \neq a} W_{i,v_i}$  is independent of  $v$  and hence

$$(\nabla F)_{ab} = \sum_{v: v_a=b} f(v) \quad (56)$$

In a single-step optimisation procedure, the value of  $v_a$  is set to

$$v_a = \operatorname{argmin}_b \left\{ (\nabla F)_{ab} \right\} = \operatorname{argmin}_b \left\{ \sum_{v: v_a=b} f(v) \right\} \quad (57)$$

In general, this is a sensible heuristic – setting one of the elements in a uniformly-chosen tree to be equal to its optimal value will often decrease the objective. Fig. 3a shows how it can successfully recover the optimal tree from an even a random starting point (given a correct ordering – discussed below), which requires a large number of changes to the tree topology. However, one must use more sophisticated gradient-based algorithms to reliably find the optimal ordered tree for more complicated phylogenies.

## F. Orderings

The continuous objective function is only defined for ordered trees, which, for a given labelling of the nodes, is a subset of the whole tree space. Thus, we define the concept of an *ordering* of the nodes and changing the ordering will allow the full space of trees to be explored.

**Definition.** Suppose that the nodes correspond to taxa with names  $N_0, N_1, \dots, N_{n-1}$ . We then define an *ordering* of the nodes to be a permutation,  $\sigma$  of the set  $\{0, \dots, n-1\}$  such that the node with name  $N_i$  is processed as node  $\sigma(i)$  by the Phylo2Vec algorithm. It is necessary that the associated Phylo2Vec vector  $v(\sigma)$  is ordered.

Note that we use the phrase “node  $x$ ” to mean “the node with name  $N_x$ ” and will always be explicit if we refer to a node by its label.

**Generating an ordering from a tree.** Given a tree, it is possible to generate a possible ordering of the nodes,  $\sigma$ , as well as the associated vector  $v(\sigma)$ . We will do this by labelling the tree, again distinguishing between the leaf node names  $N_i$  and their labels, which we will call  $l(i)$ .

Consider labelling the root node as 0. Then, label the children of this node as 0 and 1. One can continue this process inductively, choosing a node, labelled  $x$ , with unlabelled children and then labelling its children as  $x$  and  $y$ , where  $y$  is the smallest unused label. Continue this process until every node has been labelled, and, as discussed above, suppose that the label of the leaf node with name  $N_i$  is  $l(i)$ .

**Claim 1:** Two nodes have the same label only if they share an ancestor with that label.

**Proof:** Suppose that this is false, and that nodes  $x$  and  $y$  have the same label,  $L$ , but do not share an ancestor with that label. Define  $a(x)$  and  $a(y)$  to be the nodes of lowest generation (that is, the nodes closest to the root) with label  $L$  such that they are ancestors of  $x$  and  $y$  respectively. Note that, by assumption,  $a(x) \neq a(y)$  and also, neither can be the root (as the root is the ancestor of all nodes). Moreover, they cannot share a parent, as the children of a parent are labelled differently. Thus, without loss of generality, one can assume that  $a(x)$  was labelled first. By definition, the parent of  $a(x)$  does not have label  $L$  and hence,  $L$  must have been the smallest unused label when node  $a(x)$  was labelled. A similar argument for  $a(y)$  shows that  $L$  must have been the smallest unused label when node  $p(y)$  was labelled. However, when node  $a(y)$  was labelled,  $L$  had been used to label  $a(x)$ , giving the required contradiction.

**Claim 2:**  $l$  is a permutation of the set  $\{0, 1, \dots, n-1\}$ .

**Proof:** Firstly, note that as there are  $n-1$  internal nodes, and a single new label is introduced every time the children of an internal node are labelled, the set of labels used (across all nodes) must be  $\{0, 1, \dots, n-1\}$ .

Suppose that leaf nodes  $x$  and  $y$  have the same label  $L$ . By the previous claim, they must share an ancestor  $a$  with that label. Define  $b$  to be the shared ancestor with the highest generation (that is, furthest from the root) such that

$b$  has label  $L$ . Then, either nodes  $x$  and  $y$  are the children of  $b$  (in which case, they have distinct labels) or they are descendants of distinct children,  $c$  and  $d$ , of  $b$ . In the second case, one can impose without loss of generality that  $c$  does not have label  $L$  and, as label  $L$  has already been used to label  $b$ , we know that all descendants of  $c$  do not have label  $L$ . Hence, in both cases, one of  $x$  and  $y$  does not have label  $L$  as required.

**Claim 3:** For each  $i \in \{0, 1, \dots, n-1\}$ , define  $x(i)$  to be the node of the highest generation with label  $i$ . Define (for  $i > 0$ ),  $y(i)$  to be the label of the parent of  $x(i)$ . Then, with ordering  $l$ , the tree is given by

$$v_0 = 0 \quad \text{and} \quad v_i = y(i) \quad \forall i > 0 \quad (58)$$

**Proof:** Firstly, note that  $v$  is ordered, as the label of a child is greater than or equal to that of its parent. Hence, as the parent of  $x(i)$  does not have label  $i$ , it must have a label strictly less than  $i$  and so  $v_i < i$  as required.

Consider constructing the tree according the “standard” right-to-left Phylo2Vec algorithm. One can then proceed by induction on the number of nodes. The case  $n = 2$  is trivial, and so suppose it holds for  $n = m$  and consider a tree with  $n = m + 1$ .

The first node,  $x$ , to be processed has label  $m$ . The parent of the node with label  $m$  cannot also have label  $m$  (as, otherwise, its other child would have label greater than  $m$ , contradicting Claim 2). Similarly, no other node in the tree can have label  $m$  and hence, the parent of  $x$  must have label  $y(m)$ . This must also be the label of its other child and hence,  $v_m = y(m)$  ensures that the node with label  $m$  merges with its sibling from the original tree (which is correct).

From this point, the tree now has  $m$  nodes, and our right-to-left construction algorithm considers the parent of the node labelled  $m$  to now be a leaf node with label  $y(m)$ . The values of  $y(i)$  for this tree are unchanged (in particular,  $y(y(m))$  depends on the label of an ancestor of the parent of node  $m$ ) and hence, by induction, the remaining values of  $v$  correctly generate the rest of the tree. Thus, the correct tree is generated by  $v$  as required.

**The number of possible orderings for a tree.** Given a tree, one can use the previous labelling algorithm to show that there are at least  $2^{n-1}$  possible orderings for the tree (as the children of each node can be labelled in either order). The exact number depends on the choice of which internal node is processed at each step (and so, a “flat” tree where the leaves have a low generation has more possible orderings than a “ladder” tree where each leaf has a distinct generation). However, in general, it will be substantially larger than  $2^{n-1}$  (we conjecture that for flat trees, it may be factorial in size) and hence there are numerous possibilities which will allow for a global minimum of the objective to be found.

## G. Queue Shuffle: generating principled ordering proposals

**The importance of well-chosen orderings.** While the number of possible orderings for the optimal tree is large, the proportion of these orderings falls quickly as  $n$  increases. An estimate for this proportion is

$$\text{Proportion of optimal orderings} \approx \frac{\text{Trees per ordering}}{\text{Total trees}} = \frac{(n-1)!}{(2n-3)!!} \quad (59)$$

which is exponentially decreasing in  $n$ . The exact value will depend on the “flatness” of the optimal tree. Thus, it is crucial to efficiently explore the space of possible orderings to find the optimal tree, as the number of uniformly chosen orderings needed to find the optimal tree will quickly become computationally impractical.

One way to increase efficiency is to ensure that the previous best tree is in the new space of ordered trees. That is, suppose that  $\mathcal{T}$  is the optimal ordered tree for the current ordering. The algorithm in the previous section provides a method for choosing a new random ordering, by randomising the order in which nodes are processed and randomising which of the children is given the same label as their parent.  $\mathcal{T}$  will still be in the space of ordered trees, and hence re-optimising in this new ordered space will not increase the objective value (provided the true optimal ordered tree is found).

However, even choosing the new ordering from a uniform distribution over the space of orderings containing  $\mathcal{T}$  will lead to inefficient optimisation as  $n$  grows. In the optimisation scheme used in this paper, we use the topology of  $\mathcal{T}$  to further inform the distribution of the next ordering that is proposed. The true optimal tree is likely to be reasonably “close” to  $\mathcal{T}$  (especially after a few initial iterations of the algorithm) and so it is important to choose a new ordering such that allows for a thorough exploration of the space of these “close” trees.

**Asymmetry of ordered tree spaces.** A key feature of the Phylo2Vec construction that can be exploited to make sensible ordering proposals is the “asymmetry” of ordered tree space. That is, in a uniformly chosen tree from an ordered tree space, nodes with low labels are likely to be closer to the root.

This can be shown as follows. Define  $g_k^m$  to be the expected distance from the root of the node labelled  $m$  in a tree with  $k$  nodes. Then, from our left-to-right construction algorithm,

$$g_{k-1}^k = \sum_{m=0}^{k-2} \frac{1}{k-1} (1 + g_m^{k-1}) \quad (60)$$

as adding node  $v_{k-1} = m$  means that the path length between node  $k-1$  and the root will be one more than the path length of between  $m$  and the root. If  $v_{k-1} = m$ , it will also increase the path length between node  $m$  and the root by 1 and so

$$g_m^k = \frac{k-2}{k-1} g_m^{k-1} + \frac{1}{k-1} (g_m^{k-1} + 1) = g_m^{k-1} + \frac{1}{k-1} \quad (61)$$

The initial conditions of this system are that

$$g_0^2 = g_1^2 = 1 \quad (62)$$

as in a two-node rooted tree, the leaves are distance 1 from the root. Given the harmonic sum function

$$H(m) = \begin{cases} \sum_{j=1}^m \frac{1}{j} & \text{if } m \geq 1 \\ 1 & \text{if } m = 0 \end{cases} \quad (63)$$

we claim that the solution to this system is

$$g_m^k = H(k-1) + H(m) - 1 \quad (64)$$

where  $H(0) = 0$ . Note that this holds for  $k = 2$  as  $H(1) = H(0) = 1$ . Moreover, under the inductive hypothesis that it holds for  $k-1$ ,

$$g_m^k = g_m^{k-1} + \frac{1}{k-1} = H(k-2) + H(m) - 1 + \frac{1}{k-1} = H(k-1) + H(m) - 1 \quad (65)$$

and

$$g_{k-1}^k = \sum_{m=0}^{k-2} \frac{1}{k-1} (1 + g_m^{k-1}) \quad (66)$$

$$= \sum_{m=0}^{k-2} \frac{1}{k-1} (1 + H(k-2) + H(m) - 1) \quad (67)$$

$$= \sum_{m=0}^{k-2} \frac{1}{k-1} (H(k-2) + H(m)) \quad (68)$$

$$= H(k-2) + \frac{1}{k-1} \sum_{m=0}^{k-2} H(m) \quad (69)$$

$$= H(k-1) + \frac{1}{k-1} \sum_{m=1}^{k-2} \sum_{j=1}^m \frac{1}{j} \quad (70)$$

Now,

$$\sum_{m=1}^{k-2} \sum_{j=1}^m \frac{1}{j} = \sum_{j=1}^{k-2} \sum_{m=j}^{k-2} \frac{1}{j} = \sum_{j=1}^{k-2} \frac{k-1-j}{j} = (k-1)H(k-2) - (k-2) \quad (71)$$

and hence

$$g_{k-1}^k = H(k-1) + H(k-2) - \frac{(k-2)}{(k-1)} = H(k-1) + H(k-1) - 1 \quad (72)$$

as required.

Thus, the expected distance from the root grows harmonically as the label increases. For large trees, the node with label  $n-1$  has an expected distance from the root of approximately twice the expected distance from the root of the node label 0. This property is noticeable even for small trees – if  $n = 10$ , then  $g_9^{10}/g_0^{10} = 1.65$ .



**Queue Shuffle.** Our ordering proposal algorithm, *Queue Shuffle*, exploits this asymmetry to improve the efficiency with which we explore different orderings. In BME, the dominant contribution to the objective function generally comes from the nodes which are closest to the root (as these will have larger  $D_{ij}$  values than the order nodes). Thus, it is reasonable to expect that the true outgroups will be close to the root in the optimal tree in any ordering and, therefore, nodes close to the root should be given low labels in our new ordering.

Queue Shuffle uses a version of the previously discussed ordering algorithm such that the set of internal nodes with a given generation (that is, a given distance from the root) are processed consecutively. That is, we begin by processing all nodes with generation 0 (i.e., the root), then all internal nodes with generation 1, then all internal nodes with generation 2, and continue in this fashion until all internal nodes have been processed.

Algorithmically, this can be achieved by a “queue” of internal nodes to be processed. When an internal node is processed, any of its children that are also internal nodes are added to the back of this queue. Thus, the queue is always in ascending order of generation, and it is simple to show that this ensures the required property.

A crucial feature of this queue is that the child given the same label as its parent is placed *ahead* of the other child in the queue. This ensures that one can, in some way, control the order of processing by choosing the labelling of the children of each node. Moreover, it is vital for the theoretical result presented in the following section.

To add randomness into the labelling procedure, every time an internal node is processed, we randomly choose which child is given the label of their parent, and which child is given the next available label. This provides  $2^{n-1}$  possible orderings for each tree. This stochasticity is helpful in ensuring that the algorithm does not get stuck – as discussed in the subsequent section, it ensures that a large class of similar trees will be considered after a small number of ordering proposals.

**The Swapping Property.** Queue Shuffle is an extremely powerful algorithm, as it allows for great flexibility in exploring tree space, while also keeping a sense of continuity between the sets of ordered trees under consideration. This is exemplified by the *Swapping Property*, which is the fact that subtrees attached to internal nodes sharing an edge can be swapped with probability at least  $\frac{1}{4}$ , irrespective of the total number of nodes in the tree.

This property is illustrated in Fig. 2 and formalised in Theorem 1. To do this, it is necessary to have the following definitions

**Definition:** Define  $\tau(\sigma)$  to be the space of possible trees given an ordering  $\sigma$ .

**Definition:** For a tree  $\mathcal{T}$ , define  $Q(\mathcal{T})$  to be the random ordering generated by Queue Shuffle.

**Definition:** Finally, define two internal nodes to be *joined* if they share an edge.

**Theorem 1:** Consider a tree  $\mathcal{T}$ . Choose two joined internal nodes,  $i$  and  $j$  and suppose without loss of generality that  $i$  is the parent of  $j$ . Suppose that the other child of  $i$  is the root of a subtree  $\mathcal{S}_i$ , and that a child of  $j$  is the root of the subtree  $\mathcal{S}_j$ . Finally, generate  $\mathcal{T}'$  from  $\mathcal{T}$  by swapping  $\mathcal{S}_i$  and  $\mathcal{S}_j$ . Then,

$$\mathbb{P}\left[\mathcal{T}' \in \tau\left(Q(\mathcal{T})\right)\right] \geq \frac{1}{4} \quad (73)$$

To facilitate the proof, it is first helpful to prove two lemmas.

**Lemma 1.1:** For a given permutation  $\sigma$ ,

$$\mathbb{P}\left[Q(\mathcal{T}) = \sigma\right] \in \left\{0, \frac{1}{2^{n-1}}\right\} \quad (74)$$

**Proof 1.1** Suppose that every (internal and external) node in  $\mathcal{T}$  is assigned a fixed unique position, such that one can consistently define a “leftmost” and “rightmost” node from a pair of nodes. Then, the randomness in the Queue Shuffle algorithm can be represented by a uniform random vector  $\mathbf{r} \in \{0, 1\}^{n-1}$  such that when the  $m^{\text{th}}$  internal node is processed, the leftmost child is given the same label as its parent if and only if  $r_{m+1} = 1$ . Each distinct  $\mathbf{r}$  results in a distinct ordering (as, given the leaf labels, one can generate the unique labelling of the tree as a parent must have a label equal to the

minimum of the labels of its two children). Hence, each possible labelling is equally likely, giving (74) and completing the proof.

For a given permutation  $\sigma$ , define  $l_i(\sigma)$  to be the label assigned to node  $i$ ,  $l_j(\sigma)$  to be the label assigned to node  $j$ ,  $l_i^S(\sigma)$  to be the label assigned to the root of  $\mathcal{S}_i$  and  $l_j^S(\sigma)$  to be the label assigned to the root of  $\mathcal{S}_j$ . Suppose that the other child of node  $j$  is node  $c$ , and suppose it has label  $l_c(\sigma)$

This allows a further lemma to be proved about the labels of node  $i, j$  and their children.

**Lemma 1.2:**

$$\mathbb{P}\left[l_j^S(Q(\mathcal{T})) = l_i(Q(\mathcal{T}))\right] = \frac{1}{4} \quad (75)$$

**Proof 1.2:** Using the  $r$  defined in the proof of Lemma 1.1, define the random indices  $A$  and  $B$  such that  $r_A$  corresponds to processing node  $i$  and  $r_B$  corresponds to processing node  $j$ . Note that  $r_A$  and  $r_B$  are independent (though  $B$  will in general depend on  $r_A$ ).

Now, suppose without loss of generality that  $j$  is the leftmost child of  $i$  and that the root of  $\mathcal{S}_j$  is the leftmost child of  $j$ . As children have labels greater than or equal to their parents,

$$\mathbb{P}\left[l_j^S(Q(\mathcal{T})) = l_i(Q(\mathcal{T}))\right] = \mathbb{P}\left[l_j^S(Q(\mathcal{T})) = l_j(Q(\mathcal{T})) = l_i(Q(\mathcal{T}))\right] \quad (76)$$

and hence

$$\mathbb{P}\left[l_j^S(Q(\mathcal{T})) = l_i(Q(\mathcal{T}))\right] = \mathbb{P}(r_A = r_B = 1) = \frac{1}{4} \quad (77)$$

which is the required result.

**Proof of Theorem 1:** Suppose for a permutation  $\sigma$  that  $l_j^S(\sigma) = l_i(\sigma)$ . Necessarily (as  $r_B = 0$ ),  $l_c(\sigma)$  was the smallest available label when processing node  $j$ , which must be bigger than the smallest available label when node  $i$  was processed (as  $j$  is the child of  $i$  and hence processed later). Thus,  $l_c(\sigma) > l_i^S(\sigma)$ .

A further important property is that, as  $r_A = 1$  (to ensure  $l_j^S(\sigma) = l_i(\sigma)$ ), node  $j$  must have been placed ahead of the root of  $\mathcal{S}_i$  in the queue. Thus, all nodes in  $\mathcal{S}_i$  are labelled either as  $l_i^S(\sigma)$  or with a label that is greater than  $l_c(\sigma)$ , as all internal nodes in  $\mathcal{S}_i$  are processed after node  $j$ . Moreover, all nodes in  $\mathcal{S}_j$  are labelled as either  $l_j^S(\sigma)$  or a label greater than  $l_c(\sigma)$  as they were processed after node  $j$ .

Define  $v$  to be the vector giving  $\mathcal{T}$  under  $\sigma$ . Then, define a new vector  $v'$  by

$$v'_m = \begin{cases} l_i^S(\sigma) & \text{if } m = l_c(\sigma) \\ v_m & \text{otherwise} \end{cases} \quad (78)$$

Then,  $v'$  is ordered as  $l_c(\sigma) > l_j^S(\sigma)$ . We now show that  $v'$  generates  $\mathcal{T}'$  by using the left-to-right construction algorithm. Note that up to the point that node  $l_c(\sigma)$  is processed by this algorithm, no nodes have appended to the edges connecting either the root of  $\mathcal{S}_i$  or  $\mathcal{S}_j$  to the tree. This holds because all other nodes in  $\mathcal{S}_i$  and  $\mathcal{S}_j$  have labels greater than  $l_c(\sigma)$ . Changing from  $v$  to  $v'$  means that the leaf node labelled  $l_c(\sigma)$  is joined to the edge connecting the root of  $\mathcal{S}_i$  rather than the root of  $\mathcal{S}_j$ . The rest of the tree is then constructed identically as the vectors  $v$  and  $v'$  are the same.

Thus, changing from  $v$  to  $v'$  involves removing the subtree rooted at  $c$  from the edge connecting  $j$  and the root of  $\mathcal{S}_j$  and regrafting it to the tree on the edge connecting  $i$  and the root of  $\mathcal{S}_i$ . This is topologically equivalent to switching  $\mathcal{S}_i$  and  $\mathcal{S}_j$ , as shown in Fig. 2.

This completes the proof as it shows that

$$\mathbb{P}\left[\mathcal{T}' \in \tau(Q(\mathcal{T})) \mid l_j^S(\sigma) = l_i(\sigma)\right] = 1 \quad (79)$$

and hence, by Lemma 1.2

$$\mathbb{P}\left[\mathcal{T}' \in \tau(Q(\mathcal{T}))\right] \geq \mathbb{P}\left[\mathcal{T}' \in \tau(Q(\mathcal{T})) \mid l_j^S(\sigma) = l_i(\sigma)\right] \mathbb{P}\left[l_j^S(\sigma) = l_i(\sigma)\right] = \frac{1}{4} \quad (80)$$

## H. Eutherian Mammal phylogeny [87]

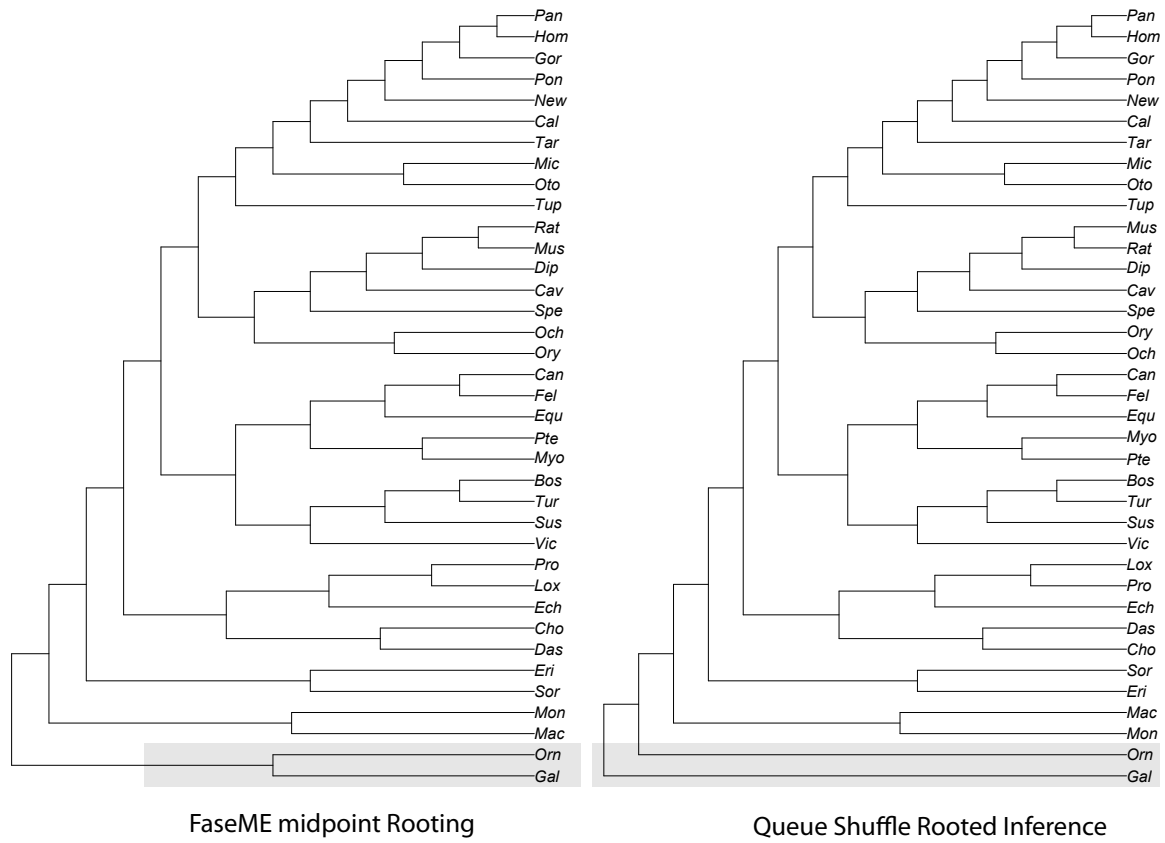


**Figure S1.** Comparison of the best unrooted FastME tree that has been midpoint rooted to an optimised rooted tree via Queue Shuffle. Queue Shuffle correctly places *Gallus gallus* as the outgroup of mammals. Branch lengths are ignored and trees are displayed as ultrametric.

## I. Convergence analysis

Figure S2 compares the performance of different optimisers (Adafactor [61], AdamW [60], RMSprop [95], and SGD) under different DNA substitutions models (JC69 [93], F81 [91], TN93 [94]) on a single optimisation step (no subsequent reordering with Queue Shuffle) for a maximum of 5000 steps. Four learning rates were considered, logarithmically spaced from 0.001 to 1.0. Whereas convergence speed appears to be independent of the chosen DNA substitution model, the results varied widely with respect to the optimisation algorithm. In particular, Adafactor optimisation produced the best performance, with increasing convergence speed as learning rates were higher.

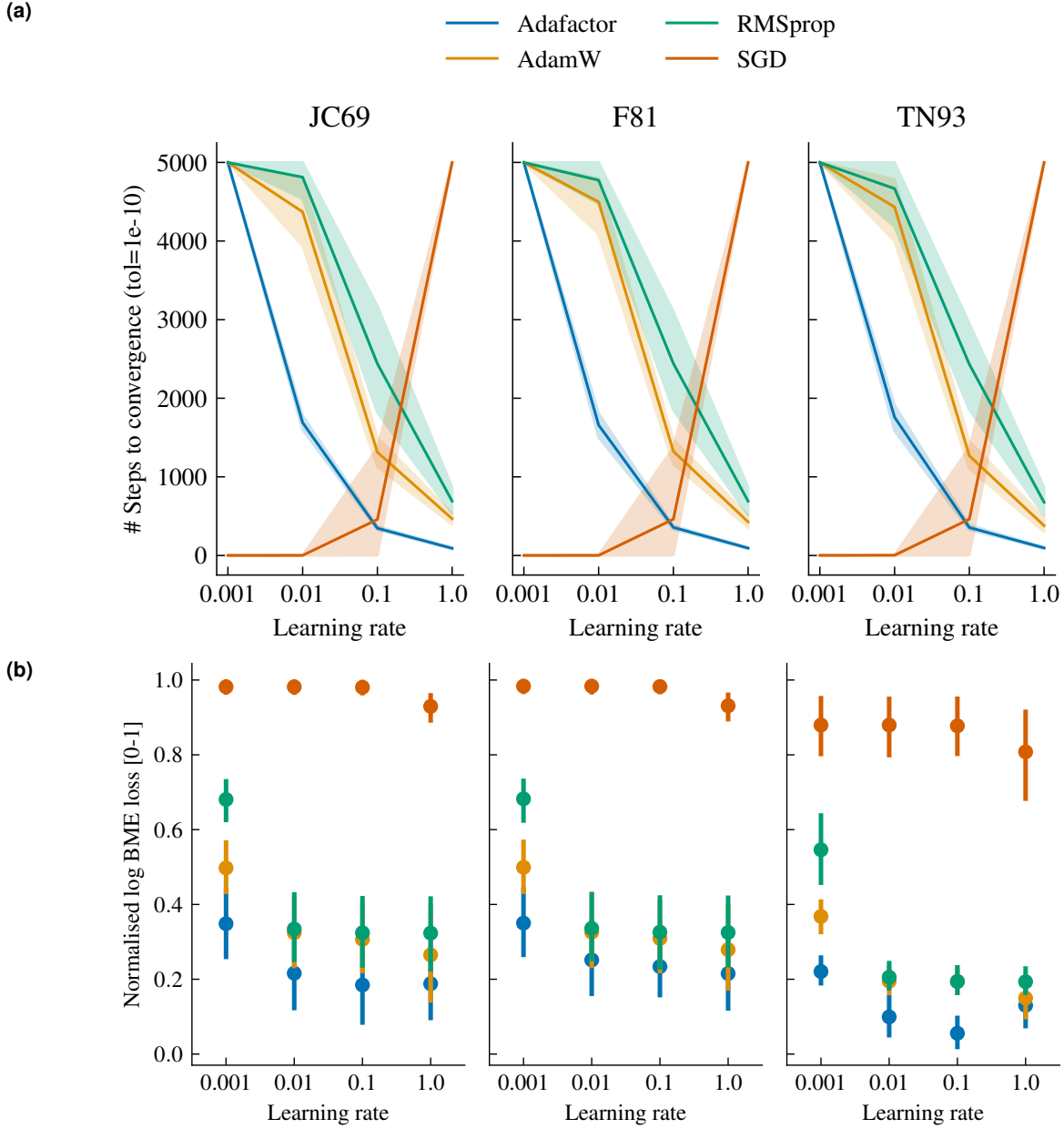


**Figure S2.** Convergence analysis of different optimisers and DNA substitution models for the datasets DS1-DS11 (see Table 1). **(a)** Number of steps needed to reach convergence (tolerance:  $1e-10$ ). **(b)** Loss reached at convergence. For each dataset, the log BME losses were scaled using min-max normalisation. Error bars denote 95% confidence intervals computed with 1000 bootstraps.